SYSTEMS, SCIENCE AND SOFTWARE

SSS-R-77-3185

SUMMARY OF THE DINING CAR TRACER-GAS CHIMNEY-PRESSURIZATION STUDIES

TOPICAL REPORT

E. Peterson
P. Lagus
K. Lie

Contract No. DNA001-77-C-0099

Submitted to:

Commander
Field Command/DNA
Kirtland AFB, New Mexico 87115

April 1977

P. O. BOX 1620, LA JOLLA, CALIFORNIA 92038, TELEPHONE (714) 453-0060

UNCLASSIFIED

SECURITY CLASSIFICATION OF THIS PAGE *(When Data Entered)*

REPORT DOCUMENTATION PAGE		READ INSTRUCTIONS BEFORE COMPLETING FORM
1 REPORT NUMBER	2 GOVT ACCESSION NO	3 RECIPIENT'S CATALOG NUMBER
4 TITLE *(and Subtitle)* SUMMARY OF THE DINING CAR TRACER-GAS CHIMNEY-PRESSURIZATION STUDIES		5 TYPE OF REPORT & PERIOD COVERED Topical 6 PERFORMING ORG. REPORT NUMBER SSS-R-77-3185
7 AUTHOR(s) E. Peterson K. Lie P. Lagus		8 CONTRACT OR GRANT NUMBER(s) DNA001-77-C-0099
9 PERFORMING ORGANIZATION NAME AND ADDRESS Systems, Science and Software P.O. Box 1620 La Jolla, California 92038		10 PROGRAM ELEMENT, PROJECT, TASK AREA & WORK UNIT NUMBERS NWET 62710H J24AAXY X983, 49
11 CONTROLLING OFFICE NAME AND ADDRESS Director Defense Nuclear Agency Washington, D.C. 20305		12 REPORT DATE April 1977 13 NUMBER OF PAGES 75
14 MONITORING AGENCY NAME & ADDRESS*(if different from Controlling Office)*		15 SECURITY CLASS *(of this report)* Unclassified 15a DECLASSIFICATION/DOWNGRADING SCHEDULE

16 DISTRIBUTION STATEMENT *(of th*

Distribution A: Approved for public release; distribution is unlimited.

17 DISTRIBUTION STATEMENT *(of the abstract entered in Block 20, if different from Report)*

18 SUPPLEMENTARY NOTES

19 KEY WORDS *(Continue on reverse side if necessary and identify by block number)*

20 ABSTRACT *(Continue on reverse side if necessary and identify by block number)*

Three tracer-gas pressurization studies were conducted in the Dining Car chimney. The objectives of these tests were to evaluate gas flow within the chimney and to measure the flow from the chimney through the surrounding material to the mesa or tunnel complex. The effective permeability and accessible void volume of the chimney and surrounding media was also determined from this data. This report describes the test procedures, test results, data analysis techniques and the distribution of material

DD FORM 1 JAN 73 1473 EDITION OF 1 NOV 65 IS OBSOLETE

UNCLASSIFIED

SECURITY CLASSIFICATION OF THIS PAGE *(When Data Entered)*

20. (cont'd.)
properties as inferred by the test data.

TABLE OF CONTENTS

LIST OF FIGURES

LIST OF FIGURES (cont'd.)

LIST OF FIGURES (cont'd.)

LIST OF TABLES

1. INTRODUCTION

Three tracer gas pressurization studies were conducted in the Dining Car chimney. The possibility that the Hybla Gold event would be conducted in the vicinity of the Dining Car chimney provided the impetus for this work. Because of the close proximity of these events, Hybla Gold cavity gas may seep into the Dining Car chimney. Should this occur, a number of questions arise. First, do these gases percolate up through the chimney, diffuse through the paintbrush and caprock and finally leak into the atmosphere above the mesa? Second, could chimney pressures become so large that hydrofracking might occur in the surrounding media and again form a leak path for the Hybla Gold cavity gas? Finally, if these first two situations do not occur, could the Dining Car chimney itself be used as the dump volume to contain the Hybla Gold cavity gases? The intent of these studies was to determine the properties of the Dining Car chimney and its surrounding to the extent that these questions could be answered.

A number of specific objectives were addressed during these tests. Most importantly, the ability of gas to flow from the Dining Car chimney to the mesa or the tunnel complex was evaluated. Effective porosity and accessible void content and their distributions throughout the chimney were determined. The extent to which the chimney material was fractured was qualitatively evaluated. In addition, increases in the Dining Car chimney pressures were measured after placing into this chimney a volume of gas equal to ∿three times the volume of non-condensible gases expected to be produced during the Hybla Gold event.

The Dining Car test proceeded as follows. Air plus a tracer gas was injected into the Dining Car chimney from the tunnel complex. Pressures and tracer gas arrival times were then measured at various points within the chimney. These data

were then used to determine chimney properties such as air void content and effective permeability. Gas samples were collected at various locations on the mesa and in the tunnel complex. These gas samples were examined for any evidence of tracer gas and provided a direct measurement of any communication between the chimney and either the mesa or the tunnel complex.

Results of the Dining Car chimney pressurization study indicate that this chimney is a competent containment vessel. There is no evidence of gas seepage from the Dining Car chimney to the mesa or to the tunnel complex. The chimney material is highly permeable and extensively fractured. Its accessible void volume is approximately twice the volume of the Dining Car cavity. If a volume of non-condensible gases equal to that produced during the Hybla Gold event is placed in this large volume, the resulting pressure increase is negligible.

In the report which follows, a brief description of the Dining Car chimney geometry and the surrounding geology will first be given. Section 3 will include a complete description of the test procedures, instrumentation and measurement techniques. Experimental results for all tests conducted on the Dining Car chimney will be presented in Section 4. Included in this section are the results of the testing carried out to determine communication between the chimney and the tunnel complex and mesa. Analytical-numerical techniques used to determine chimney properties such as accessible void content, permeability and fracture extent are presented in Section 5. A complete description of the inferred material properties is given there. A summary of all results is given in the final section.

These tests were carried out under the direction of Joe LaComb of DNA. Systems, Science and Software (S^3) performed as a consultant. In addition, S^3 was responsible for the performance of the tracer gas studies and for the

interpretation of the pressure and tracer gas results to determine properties of the chimney material. The following report summarizes the S^3 activities and results in considerable detail. To make this summary meaningful, it is, however, necessary to include some background information concerning the test itself. A minimum amount of information is therefore included on the geology, chimney geometry, test equipment, test procedures and test results. It is anticipated that DNA will provide a more complete report covering these subjects.

2. DESCRIPTION OF DINING CAR CHIMNEY AND SURROUNDINGS

The Dining Car chimney and surrounding strata are shown in Figure 1. Chimney geometry is determined from drill back information. The location of the working point is known. Positions at which the three drill holes intersect the chimney are estimated from drilling information. The remainder of the chimney geometry is extrapolated from these four known positions. Properties of the chimney material are unknown. Some approximate properties for the surrounding strata are shown in Figure 1. These material property values are given here only to illustrate the differences between the various layers.

Material property data shown in Figure 1 were taken from Reference 1. They represent TerraTek data taken from competent samples obtained from the UE12N #9 exploratory hole. Values of permeability were determined from oven dried samples and consequently are likely to greatly overestimate the gas permeability of competent material. Gas permeability data are also shown in Ref. 1 for saturated tuff. There is a gross discrepancy between dry and saturated tuff permeability with values differing by about two orders of magnitude. However, the presence of fractures in the in situ material may greatly increase the effective permeability of the formation. Preliminary testing, based on the U12E18 PS #1 hole indicate this to be the case. In fact, whole hole permeability tests conducted on the U12E18 PS #1 hole indicate the average permeability of the paintbrush material may, indeed, be very similar to the permeability of the oven dried competent material.

Interpretation of the test data is, in many cases, sensitive to the condition of the drill hole. Therefore, a detailed description of these holes will be given. The three drill holes are shown in relation to the chimney geometry in Figures 2 and 3.

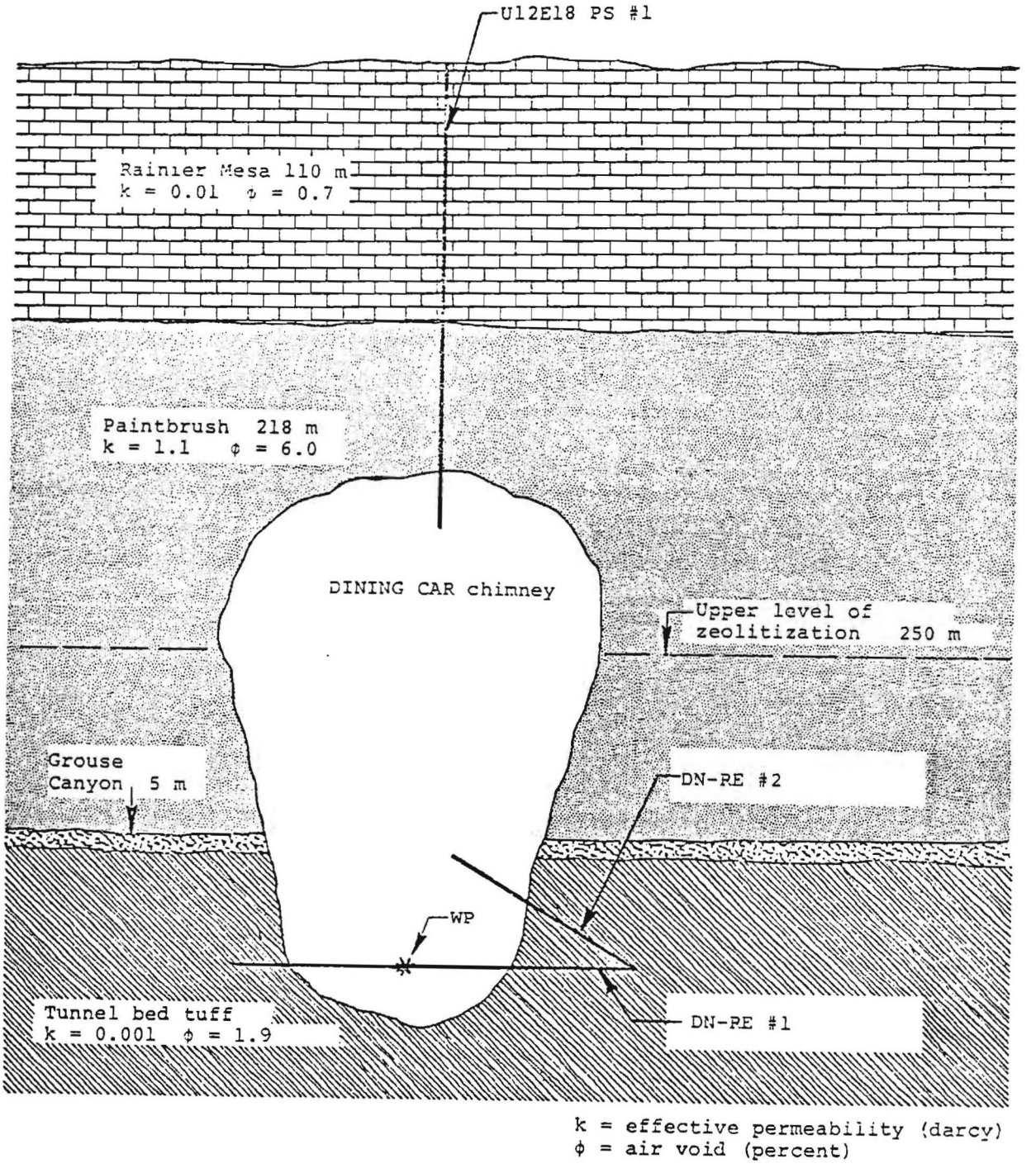

Figure 1 - Dining Car chimney geometry and surrounding geology.

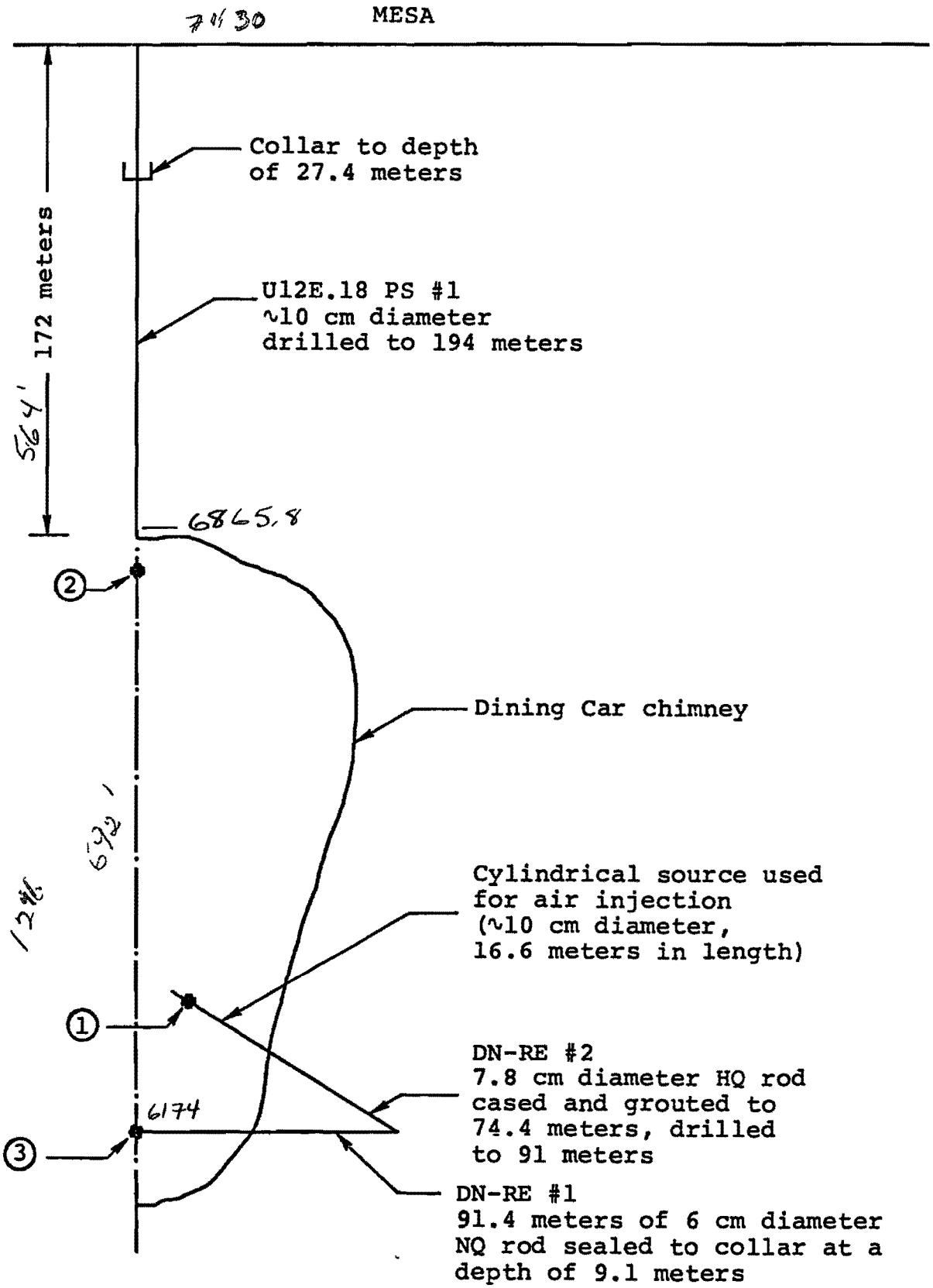

Figure 2 - Dining Car chimney showing a detailed description of all drill holes.

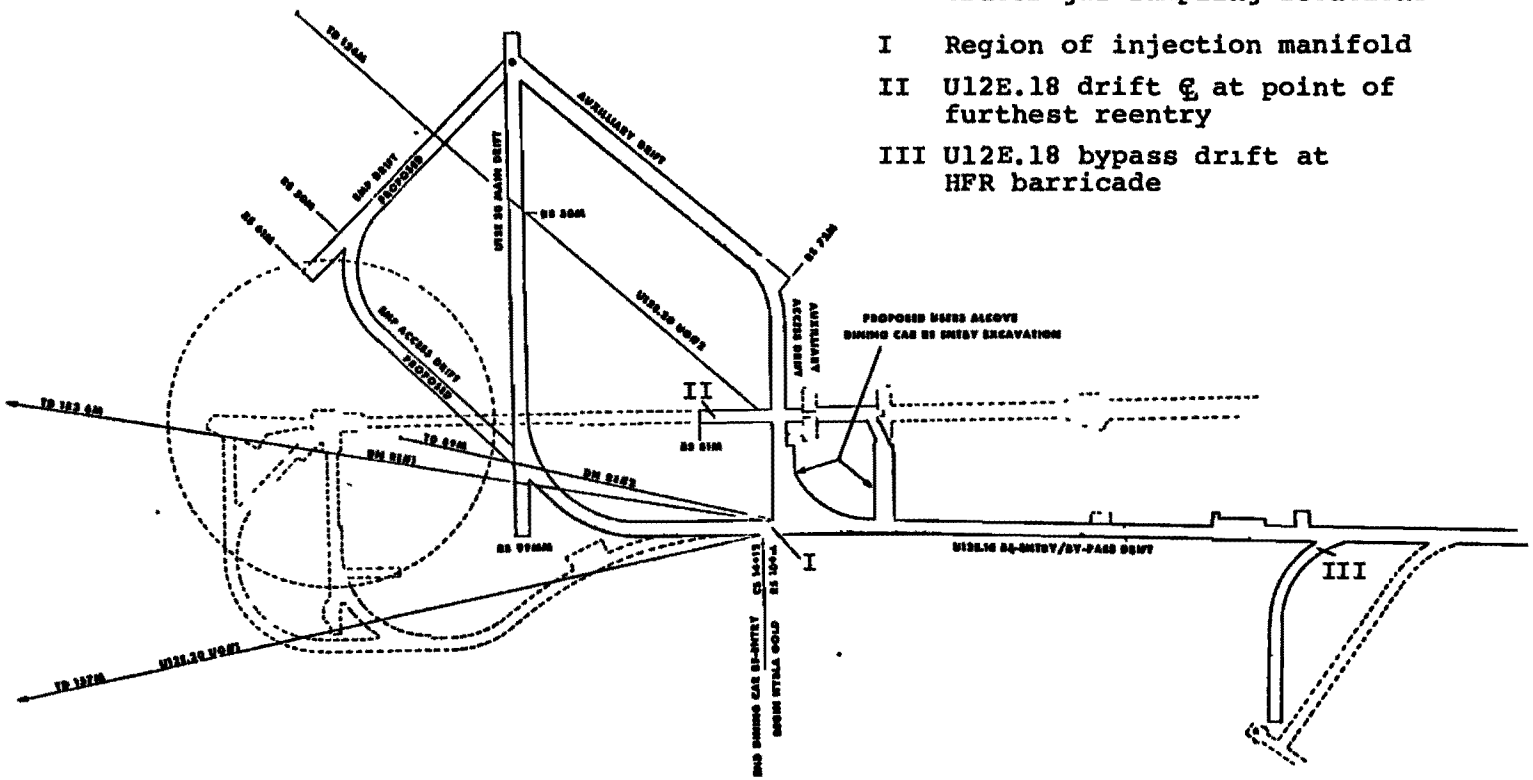

NOTE: The U12E.20 tunnel complex did not exist at the time the tracer-gas chimney pressurization studies were performed.

Figure 3 - Schematic showing Hybla Gold and Dining Car geometries and tracer gas sampling positions.

U12E18 PS #1 is a vertical hole leading from the mesa to the chimney. It has a total depth of 194 m and intersects the chimney at a depth of 172 m. During the 24 January 1977 test, this hole was uncased except for a 27.4 m collar leading down from the mesa surface into the caprock. The hole was nominally 10 cm in diameter. This hole was cased and grouted down to the top of the chimney prior to the 27 February and 1 March tests.

At the time of the 24 January test, the DN-RE #1 reentry hole extended from the U12E18 bypass drift to the working point region. The entire length of this hole was cased with 6 cm I.D. NQ drill rod which was sealed to the collar at the 9.1 m depth. Subsequent to the 24 January test, the hole was extended in length to a depth of 182.6 m. At this length, it passes completely across the bottom of the Dining Car chimney and into the media on the far side as shown in Figure 3. The portion of this hole from the working point to its end is uncased. This latter configuration existed during the 27 February and 1 March tests.

The DN-RE #2 hole began in the U12E18 bypass drift and continued into the tunnel at an angle of 30° from the horizontal. This hole was drilled to a depth of 91 m. The first 74.4 m was cased and grouted using 7.8 cm I.D. HQ rod. The remaining 16.6 m of this 10 cm diameter drill hole was left uncased and served as the source for air injection into the chimney. This cylindrical source terminated approximately 12 m from the chimney centerline.

During all tests, all holes had a 0.24 cm I.D. copper capillary tube and a 1.27 cm I.D. copper pressure tube running to the measurement points. The small tubes were used to draw gas samples from the chimney while the larger line was used for pressure measurements.

3. TEST DESCRIPTION

The tracer-gas chimney-pressurization tests proceed as follows. Air, including a tracer gas, is injected into the DN-RE #2 hole for a specified number of hours. Pressures at the source, working point (WP) and chimney top are monitored during both the pressure rise and decay periods. Tracer gas samples are periodically taken from the working point and the chimney top in order to determine tracer gas arrival times. Air samples are collected at various points on the mesa and in the tunnel complex to determine if the gas is seeping from the chimney. These data are subsequently analyzed to determine the accessible void volume, effective permeability and extent of fracturing of the chimney material.

3.1 PRESSURE MEASUREMENTS

Pressure measurements were made at points 1, 2 and 3 shown in Figure 2. Measurements were made using water manometers, mercury manometers or gages as the situation dictated. Sensitive measurements were made using water manometers capable of measuring pressures ranging from 0.07 to 20 KPa. Water manometers on the mesa were filled with a 50 percent water/ 50 percent ethylene glycol solution having a combined density of 1.05 gm/cc to prevent freezing. Recording microbarographs were placed on the mesa and in the tunnel in order to provide a record of atmospheric pressure changes. Manometer data were corrected for these changes in atmospheric conditions. Pressure data was recorded by H&N personnel throughout these tests.

3.2 FLOW RATE MEASUREMENTS

A schematic of the injection apparatus is shown in Figure 4. Air used as the carrier gas was piped from the portal to the injection site through a 15.2 cm diameter line.

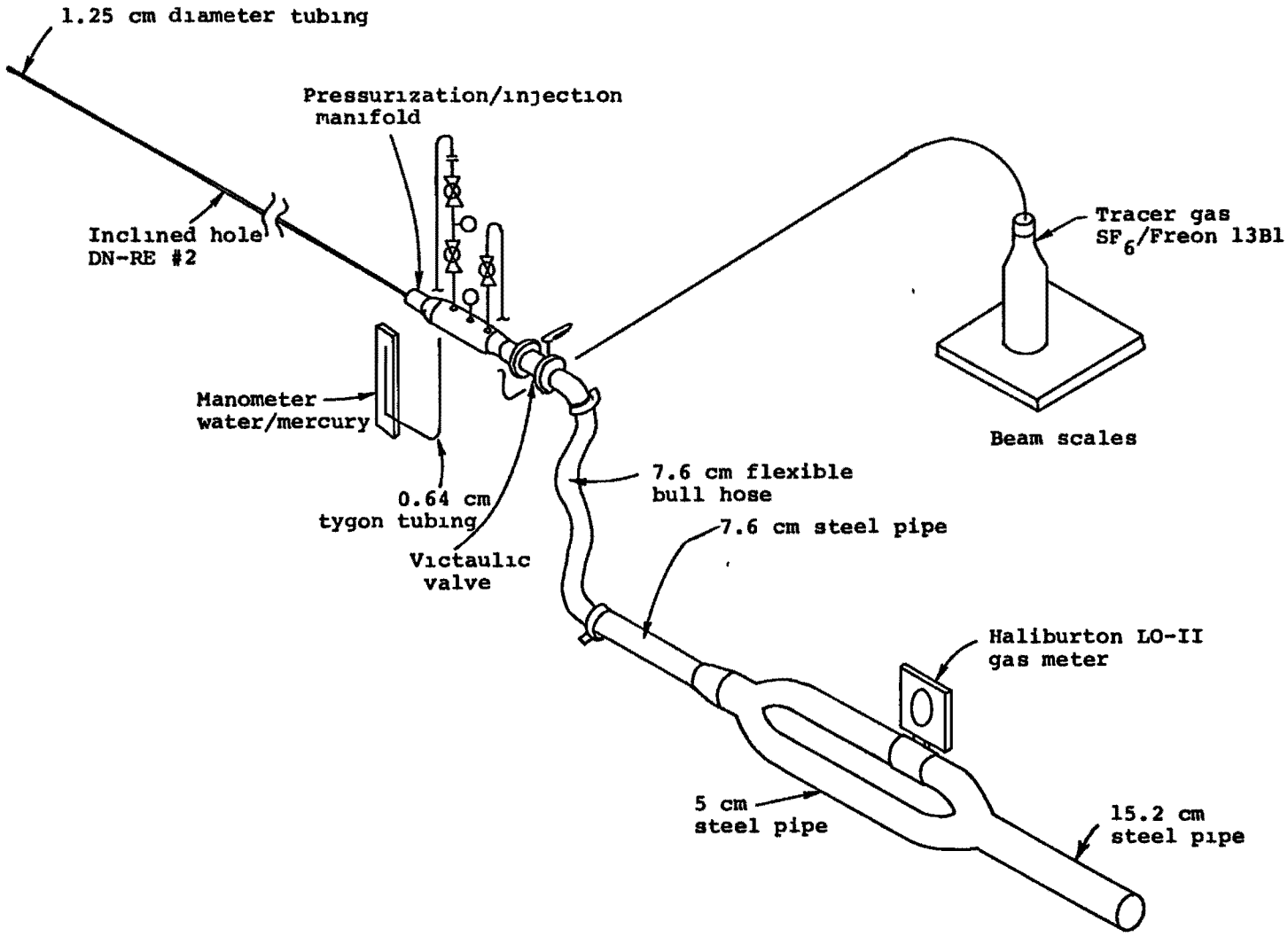

Figure 4 - Schematic showing injection apparatus.

This line was reduced to two 5 cm diameter lines prior to reaching the injection manifold. A Haliburton 5 cm diameter LO-II flowmeter was placed in one of these smaller lines. When possible, flow rates were measured using this meter which was calibrated to read standard cubic feet (SCF) of gas at a 0.51 MPa back pressure. Flow rates ranging from 11 standard cubic meters per minute (SCMM) to 110 SCMM could be read directly with this meter. The meter was equipped with an accumulator which recorded total flow. Difficulty was encountered in using the gas-driven flowmeter. The air vane which was directly in the flow was often damaged by debris flowing down the pipe. Because of the uncertainty in flowmeter operation, flow rates were also calculated based on the pressure drop along the inlet pipe. These calculations will be discussed in a later paragraph.

The tracer gas was injected into the main airstream using the manifold shown in Figure 4. Almost all joints in this manifold were welded to prevent leakage of the tracer gas into the tunnel complex. Unfortunately, a few threaded joints existed. These go from the manifold to the valves connected to the manometer lines and to the line leading to the tracer gas source. The tracer gas bottle was placed on a beam scale. Mass flow rates were determined from measurements of the bottle weight as a function of time.

Pressures were constantly monitored at the flowmeter, the injection manifold and the one-half inch line leading down to the end of the casing on the DN-RE #2 hole. These pressures were required to determine the air injection rate. A zero flow line pressure of $\sim$0.61 MPa could be obtained. Depending on the rate at which the chimney would accept gas, the full flow back pressure ranged from 0.4 to 0.55 MPa. Flowmeter readings were easily corrected for these variations in back pressure as the calibrated flow rate is simply proportional to the absolute pressure. The compressor capability at the tunnel portal was

such that, with nominal back pressures of approximately 0.4 MPa at the flowmeter, flow rates on the order of 100 SCMM could be attained.

Flow rates were also calculated based on the pressure drop along the DN-RE #2 injection hole. It was assumed that the flow from the portal into the chimney was isothermal. With this assumption, the flow rate can be calculated using Equation (1) shown below.

$$w = A \left\{ \frac{P_i \rho_i [1 - (P_e/P_i)^2]}{4f \frac{L}{D} + \ell n (P_i/P_e)^2} \right\}^{1/2} \qquad (1)$$

This equation, taken from Reference 2, describes isothermal flow of a compressible gas through a long constant area duct subject to friction. Here, w, A, P and ρ represent the flow rate, pipe cross-sectional area, gas pressure and density, respectively. Furthermore, L is the pipe length (in this case 74.4 m), d the pipe diameter, $4f$ is the friction factor for a steel pipe taken as 0.017. The subscripts i and e represent the injection manifold and the end of the casing, respectively.

When the flowmeter was working properly, flow rates calculated using Equation (1) agreed to within 10 percent with those indicated by the flowmeter. Equation (1) was therefore used to determine the flow rates when the flowmeter was inoperable.

3.3 TRACER GAS MEASUREMENTS

Gas samples were collected on the mesa, in the tunnel complex and from points within the chimney at prescribed intervals. These samples were returned to the instrumentation station located at the Dining Car surface ground zero (SGZ) or to the station located in the U12E18 reentry drift where they were

analyzed for evidence of tracer gases.

Mesa samples were taken at points shown on the grid in Figure 5. This grid was 305 m in diameter centered on the Dining Car SGZ. Sampling locations were at the 61 m, 152 m and 305 m positions on each of 12 radials oriented at 30° intervals and at the SGZ. In practice, one man carried sufficient syringes in a small basket-like container to allow him to walk two radials; one out, and then a second radial on his return to the SGZ area. At each location, replicate samples (i.e., two samples) were drawn by first aspirating the syringe and then drawing a sample approximately 1 cm above the ground. When all six sample locations had been occupied, the full basket was returned to the instrumentation station for analysis. At all times during which samples were drawn on the mesa, a Meteorology Research Inc. portable weather station was in operation. This weather station measured wind speed and direction as well as outdoor temperature. In this way it is possible to correlate observed tracer gas patterns with prevailing winds and thereby make inferences about the total amount of tracer gas observed, and also to assess the possibility that any observed tracer gas was a spurious leak contributed by a tunnel portal rather than an actual leak to the surface of the mesa.

Air samples were collected in the tunnel complex at the positions shown in Figures 3 and 6. Two samples were taken at chest height near each location marked on the tunnel wall. A set of syringe samples would be collected in a small basket-like container and returned to the instrumention station in the U12E18 reentry drift for analysis.

Gas samples were taken from within the chimney at points ② and ③ shown in Figure 2. During each sampling, two 1000 cc sealable plastic bags were filled with gas drawn from the chimney through the 0.25 cm capillary line using a vacuum pump. The first bag was drawn to clear the line of gas which had entered

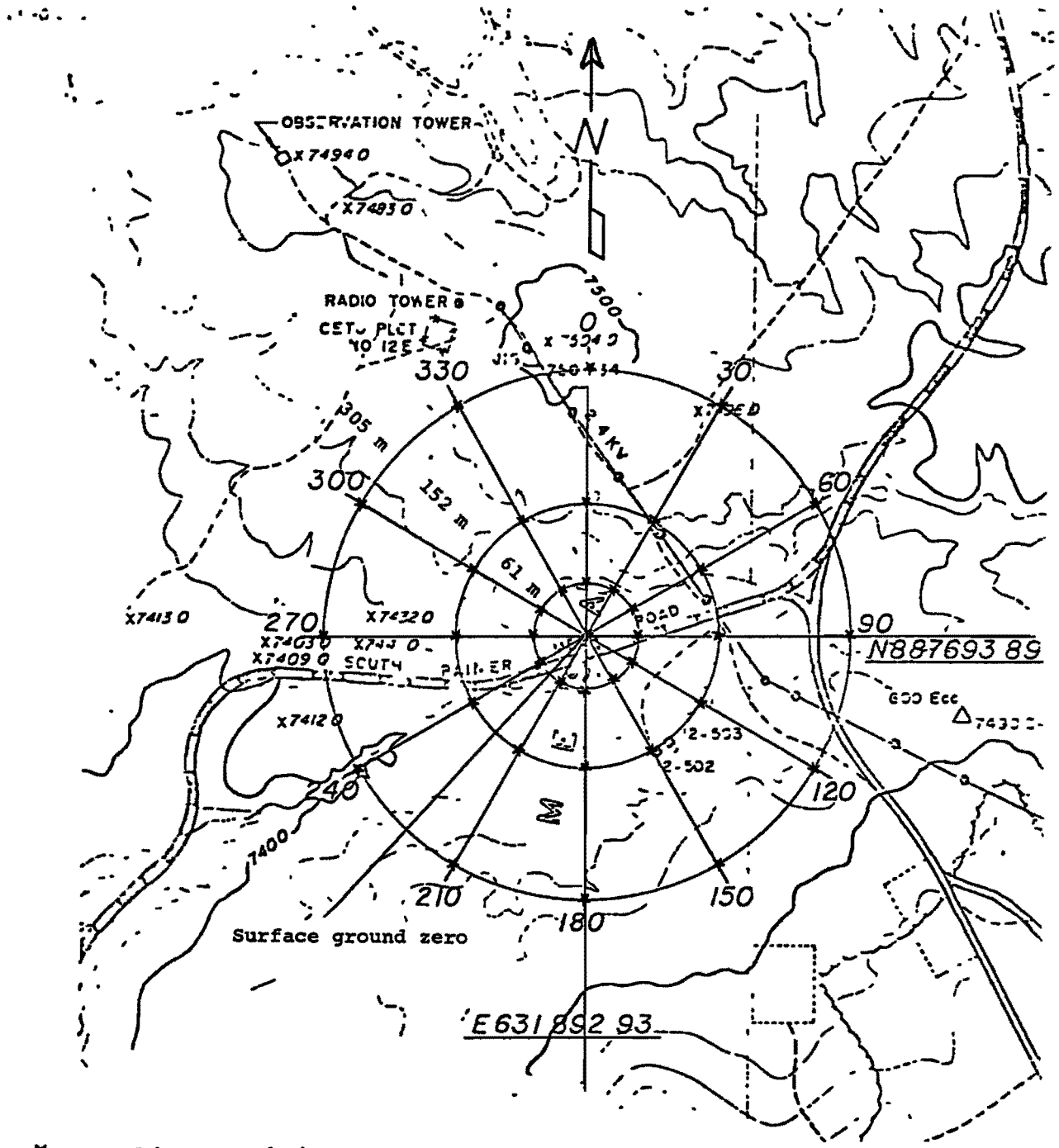

* Sampling positions

Figure 5 - Mesa plot plan showing sampling grid centered on the surface ground zero (SGZ).

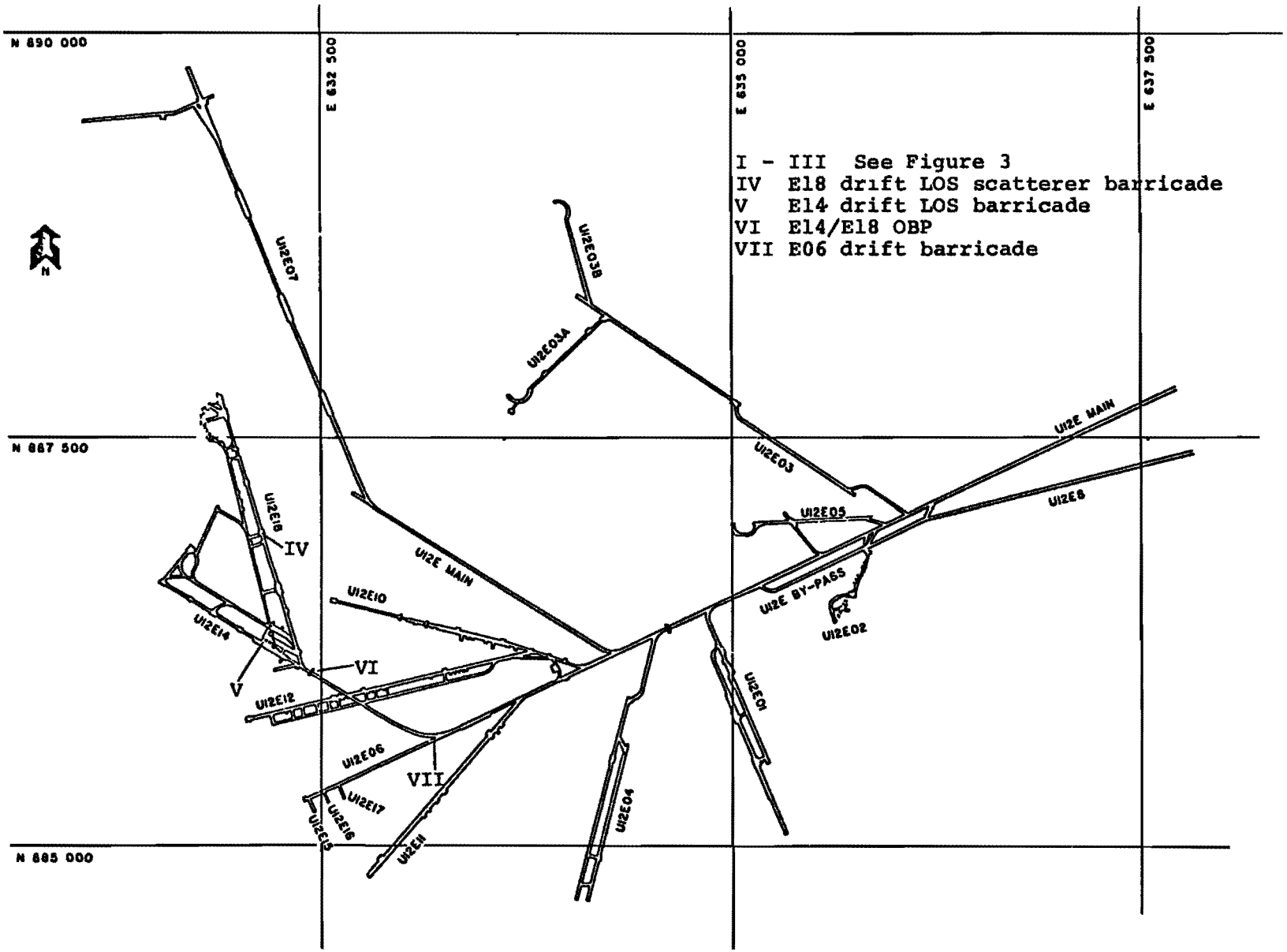

Figure 6 - U12E tunnel layout showing tracer gas sampling stations.

while taking the preceding sample. Two syringe samples were drawn from the second bag and used for analysis purposes.

Gas samples were obtained using disposable sampling bags and disposable 12 cc polypropylene syringes with 23 gage needles. To eliminate any possibility of cross-contamination or spurious effects due to gas leakage, a syringe was used only one time. Air bags were reused only if the analysis indicated the absence of tracer gas. Once a bag had been exposed to SF_6 or Freon 13B1, it was disposed.

Each syringe was labeled with a gummed sticker on which was noted the time and position at which the syringe sample was obtained. This sticker was removed when the sample was analyzed, and affixed to the strip chart output to identify the given chromatogram. Two syringe samples were drawn at each sample location to allow a measure of reproducibility. A suspicious indication of tracer gas would not be considered real unless it appeared in both sample measurements.

Air samples were analyzed for evidence of tracer gas using the Systems, Science and Software (S^3) electron capture gas chromatograph shown schematically in Figure 7. Samples to be analyzed were injected into the instrument by means of the disposable syringes. Injection was through a rubber septum located on the sample port. This septum prevents spurious contaminants from diffusing into the chromatograph and producing anomalous signals.

The S^3 gas chromatograph utilizes the high electron affinity of gases with halogen group elements to provide a measureable signal. The heart of the instrument is the column. It separates the various gaseous components of a sample by selectively slowing down some gases relative to others. The column can be thought of as a device to elute the distinct components in a gas sample in a definite order. When monitoring SF_6 plus selected Freons, experience has shown that a column

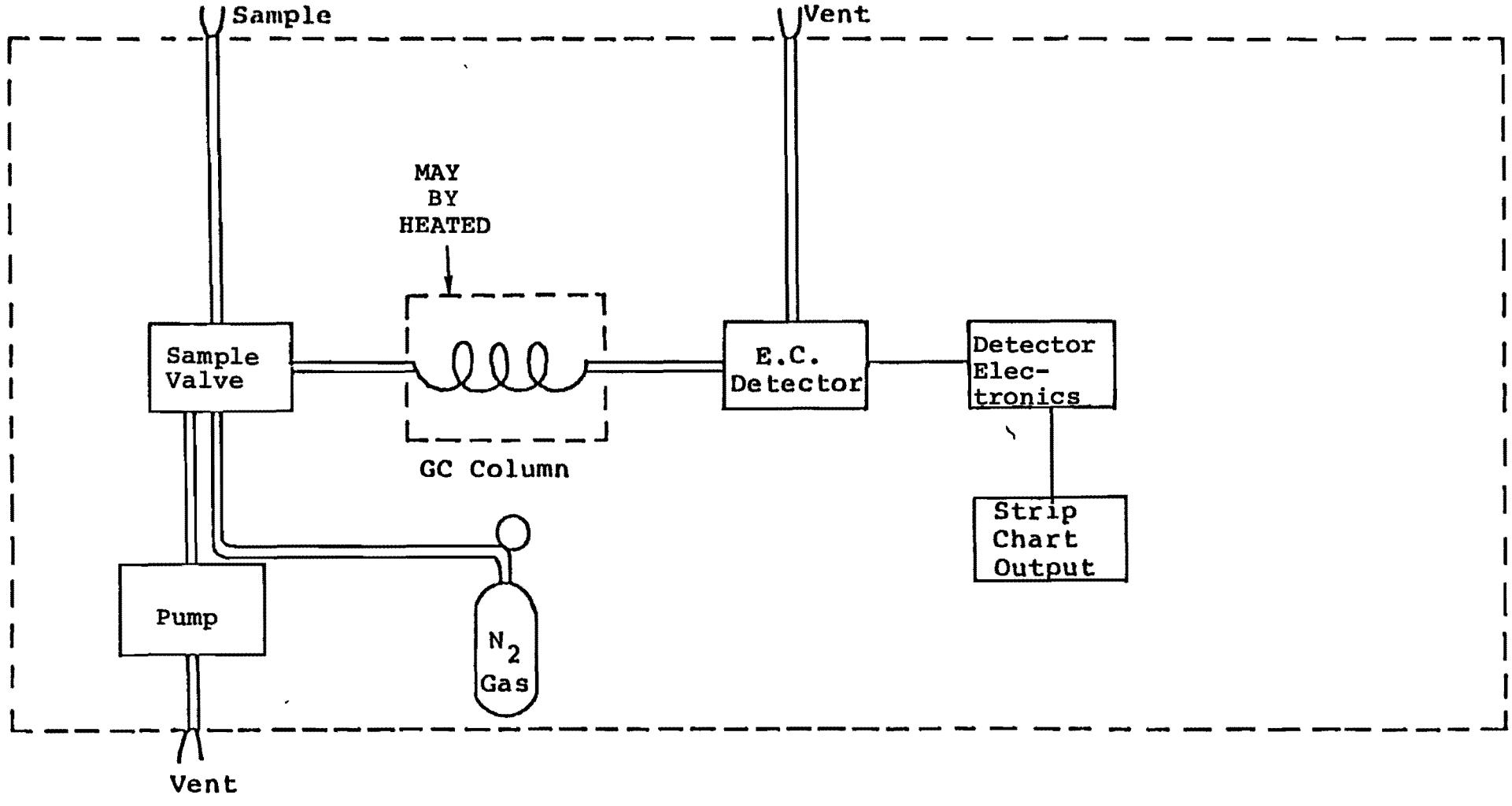

Figure 7 - Schematic drawing of electron capture gas chromatograph.

consisting of one of the Porapaks* provides excellent separation as shown in Figure 8. The ultimate sensitivity of the S^3 tracer gas monitor to SF_6 and Freon 13B1 used in these tests is $\sim 10^{-12}$ and $\sim 10^{-11}$ parts tracer gas per part air, respectively.

During the course of each series of measurements, a set of standard gas mixtures would be injected into the monitor from time to time to provide fiducial peaks on the chromatogram. These fiducials allow one to have greater confidence in one's ability to pick a given arrival as a particular tracer gas. In general, it should be emphasized that these standard mixtures were not meant to be used for quantitative analysis, but rather to provide qualitative arrival times of the various tracer gas species being monitored during the course of these experiments.

*Registered Trademark of Waters Associates.

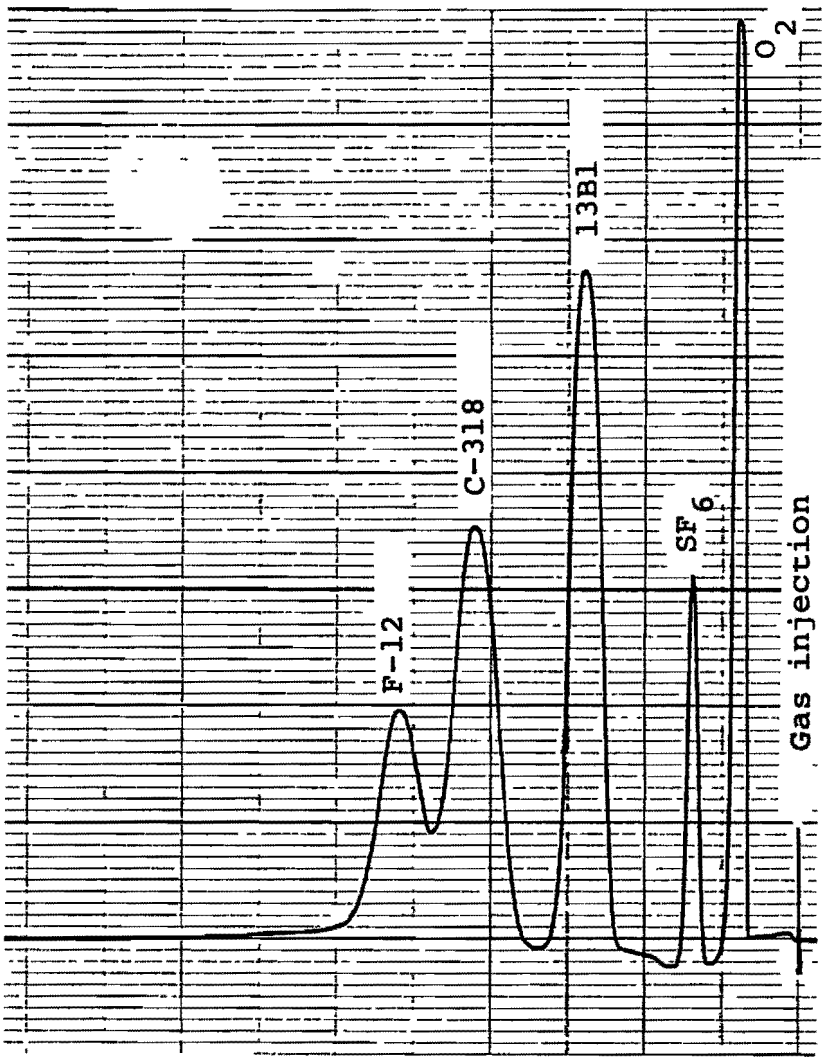

Figure 8 - Chromatograph response showing separation of various tracer gases on a 1 meter Porapak Q column.

4. EXPERIMENTAL TEST RESULTS

Three tracer gas pressurization tests were conducted in the Dining Car chimney. The first of these tests began on 24 January. The objective of that test was to determine the properties of the Dining Car chimney and surrounding materials and to evaluate possible communication between the chimney and mesa or tunnel complex. A second test was conducted on 27 February. During this second test, a volume of air equal to approximately 3 times the amount of non-condensible gases expected to be produced during the Hybla Gold event was injected into the Dining Car chimney. The intent was to evaluate the capability of the Dining Car chimney to contain or accept the amount of non-condensibles produced by Hybla Gold. A third test was initiated on 2 March. This test was conducted to clarify certain anamolous behavior observed during the 24 January test. The 2 March test was therefore a repeat of the 24 January test. In the following section, the Hybla Gold simulation test conducted on 27 February will first be discussed. Following this, the results of the chimney pressurization tests of 24 January and 2 March will be presented.

4.1 HYBLA GOLD SIMULATION TEST

The objective of the Hybla Gold simulation test was to evaluate the capability of the Dining Car chimney to accept and contain the $\sim 3.0 \times 10^3$ SCM of non-condensible gases which may be produced during the Hybla Gold event.* During this test, pressure and tracer gas arrival times were monitored at points ①, ② and ③ shown in Figure 2. Gas samples were collected in the tunnel complex and on the mesa at positions shown in Figures 3, 5 and 6. These samples were analyzed for any evidence

*This volume assumes the zero room walls are made of steel and the zero room itself is filled with fiberglass. Larger or much smaller values are expected for different initial conditions.

of tracer gas, the presence of which would indicate communication of the chimney with these regions.

Air containing sulphur hexafluoride (SF_6) was injected into the Dining Car chimney on 27 February for a 106 minute period. The flowmeter indicated a flow rate of 80.1 SCMM. The flowmeter appeared to be operating properly during this test, therefore the flowmeter values are assumed to be correct. As shown in Figure 9, approximately 13.6 Kg of SF_6 were injected during this test. This corresponds to a concentration of approximately 2.5×10^{-4} parts SF_6 per part air, assuming a uniform injection rate. Recall the instrumentation used to analyze gas samples is sensitive to approximately 10^{-12} parts SF_6 per part air.

Changes in chimney pressure resulted from injection of this volume of air are shown in Figure 10. Pressure differentials shown are with respect to the local ambient pressure which varies slightly with altitude. Injection of this volume of gas at a relatively rapid rate is seen to increase the pressure in the injection region of the chimney by approximately 4 kPa. At the top of the chimney, the pressure increased only 2.6 kPa. Within approximately 5 hours after completion of the air injection, the chimney pressure had become uniform at 1.7 kPa. At this time, the pressure decay rate had become very slow. Conspicuous by its absence in Figure 10 are pressure measurements taken at the working point. Pressures were monitored at the DN-RE #1 hole, however, there was no indication of pressure arrival. These data imply there is no communication between the injection region and working point region of the Dining Car chimney.

Chimney pressurization began at 1409 on 27 February. Gas sampling on the mesa began at 2100 on 27 February. Additional samples were collected at 0900, 1300, 1700 and 2100 on 28 February and at 0100, 0500 and 0900 on 1 March. No

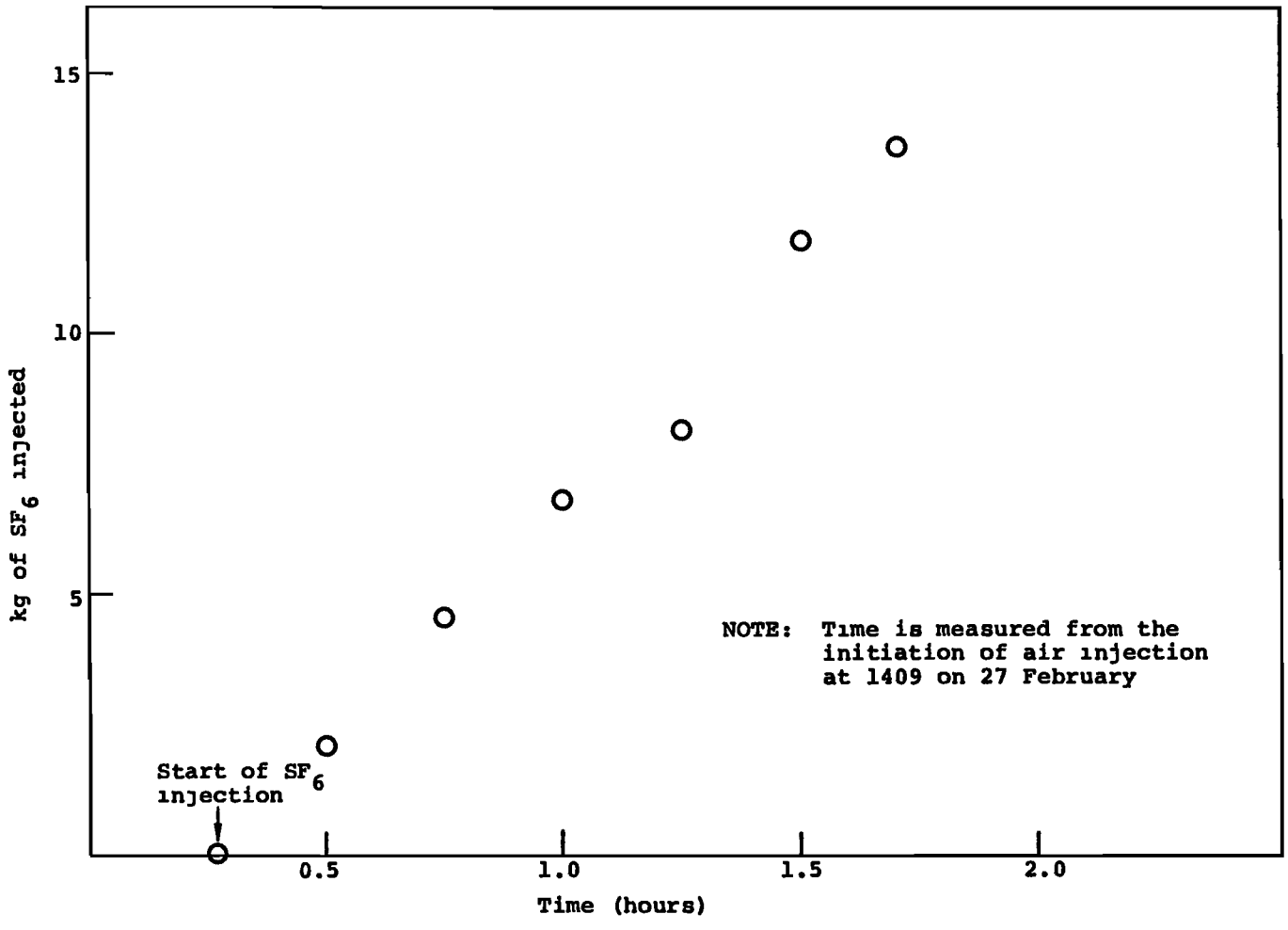

Figure 9 - SF_6 injection rate during the 27 February Dining Car chimney pressurization test.

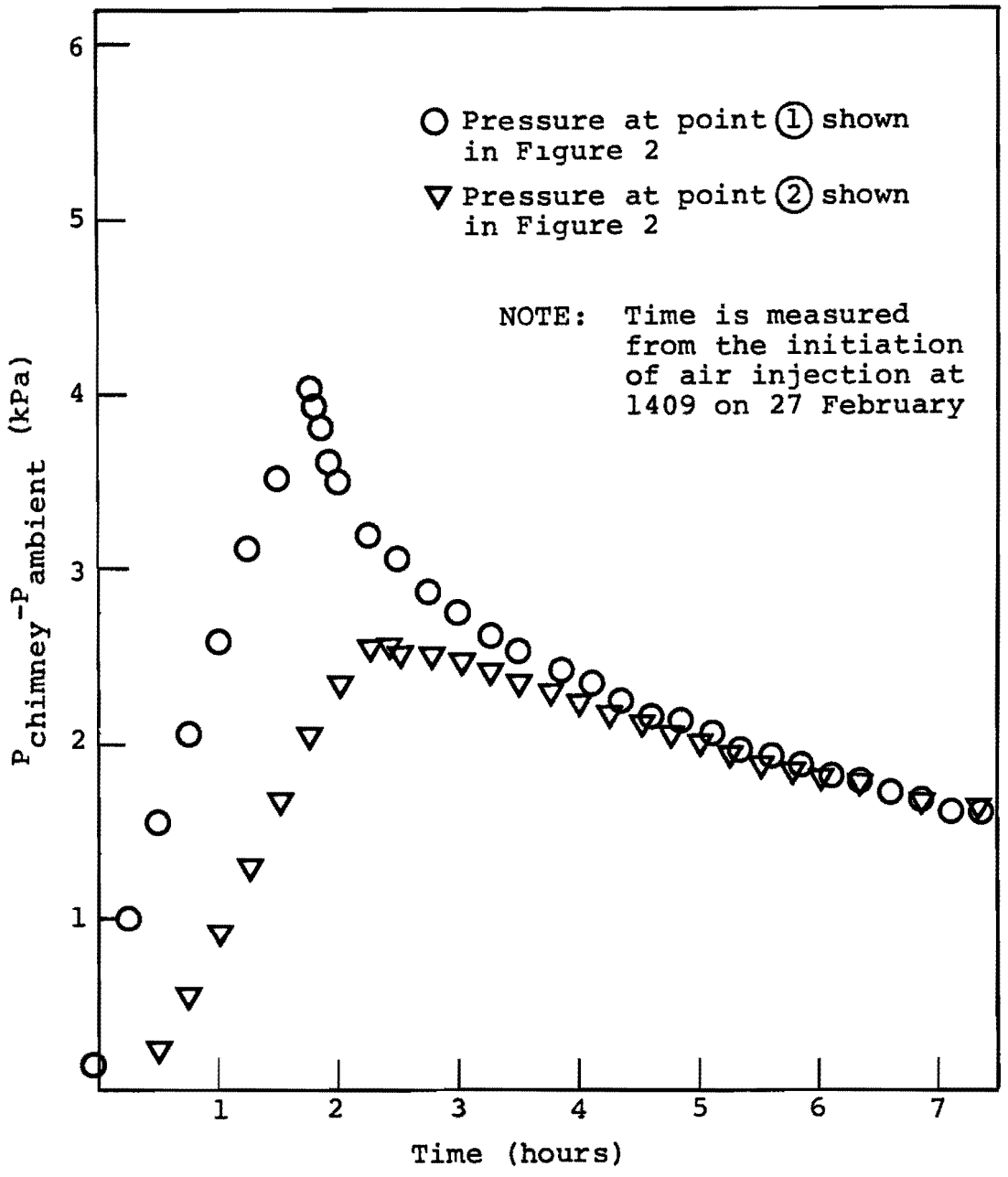

Figure 10 - Measured Dining Car chimney pressure history during the Hybla Gold simulation test.

traces of SF_6 or Freon 13B1 (used during the 24 January test) were found in these samples. Gas samples were periodically drawn from the top of the chimney through the U12E18 PS #1 hole. Analysis indicated the injected tracer gas failed to reach the top of the chimney. Gas samples taken from the DN-RE #2 hole were also free of SF_6.

An attempt was made during the 27 February test to determine if gases could possibly leak from the Dining Car chimney into the tunnel complex. Previous experience had indicated that gas in the tunnel complex is rapidly homogenized because of the ventilation system and train traffic in the small diameter tunnels. As a result of this rapid homogenization, it had, on previous occasions, been impossible to determine the source of tracer gases which had entered the tunnel complex. To alleviate this problem, all train traffic was halted and the tunnel ventilation was shut down during the 27 February test. During this test, gas samples were collected at prescribed time intervals at the tunnel positions shown in Figures 3 and 6.

Unfortunately, the threaded joints in the line between the SF_6 bottle and the injection manifold could not be made tight enough to prevent a small leakage of SF_6. During the pressurization phase of this test, SF_6 continuously leaked from this line. SF_6 levels were therefore carefully monitored in the vicinity of the injection manifold in order to estimate the background SF_6 level introduced into the tunnel complex as a result of this leak. Measurable levels of SF_6 were eventually found in the U12E18 reentry drift, however, there was no indication of any other source for this SF_6 than the injection line running from the SF_6 bottle to the main manifold.

It should be noted that even in the absence of tunnel ventilation and train traffic, there seemed to be a slight draft from the chimney back toward the portal along the U12E18

reentry drift. The SF_6 cloud slowly moved up this drift and by 1800 on 27 February, SF_6 was detectable in the U12E18 reentry drift at a location equivalent to the position of the scatterer barricade which is approximately 90-120 m from the injection manifold.

In summary, when a volume of gas equal to three times the possible Hybla Gold non-condensibles is placed in the Dining Car chimney, the resulting pressure increase is approximately 5 kPa. This gas does not penetrate through the paintbrush and caprock to the mesa nor does it seep into the U12E18 tunnel complex.

4.2 CHIMNEY CHARACTERIZATION STUDY

4.2.1 24 January Test

In the 24 January test, gas flow from the Dining Car chimney through the surrounding material to the mesa and tunnel complex was studied. The accessible void volume, effective permeability and fracture extent of the chimney material was also investigated. During this test, a large volume of air ($\sim 10^5$ m^3), containing Freon 13B1 as a tracer gas, was injected into the chimney to produce the elevated pressures needed for these studies. Chimney material properties were determined using tracer gas arrival and pressure data obtained within the chimney at points shown in Figure 2. Communication between the chimney and its surroundings was evaluated by analyzing air samples collected on the mesa and in the tunnel complex for evidence of Freon 13B1.

Pressurization began at 1800 on 24 January through the DN-RE #2 hole. A flow rate of 90.6 SCMM was indicated by the flowmeter. Calculations based on the pressure drop along the DN-RE #2 hole indicated a rate of 87.8 SCMM, thus confirming the flowmeter reading. Approximately 18.2 Kg of Freon 13B1

(bromotrifluoromethane) were injected into the Dining Car chimney during the first one-half hour of pressurization at a concentration of $\sim 10^{-3}$ parts 13B1 to one part air.

The pressure history within the chimney throughout the duration of this test is shown in Figure 11. The first pressure and decay cycle provides sufficient data to determine properties of the chimney and surrounding material. The second and third pressurizations were required to maintain pressures high enough to force gas from the chimney to the mesa. Useful pressure data could not be obtained from the DN-RE #1 hole leading to the working point region. Throughout the test, this hole filled with water at a rate corresponding to a pressure increase of 3 kPa per hour. During the first 20 hours of pressurization, $\sim 1.1 \times 10^{5}$ m^3 of air were injected into the Dining Car chimney. Additional volumes of 3.7×10^{4} and 2.3×10^{4} m^3 were added during the second and third pressurization periods, respectively.

A summary of the results of the analysis of gas samples taken on the mesa during the 24 January test are shown in Table 1. Recall from Figure 11 that pressure arrival occurred at the top of the chimney in less than 1/2 hour after the onset of pressurization. Low concentrations ($\sim 10^{-10}$) of tracer gas were detected at the top of the chimney 6 1/2 hours after the pressurization began. There was no evidence of tracer gas on the mesa during 25 January. During the first sweep on 26 January, tracer gas was found at two positions on the mesa as shown in Figure 12. A second sweep at 1400 on 26 January indicated significant quantities of Freon 13B1 on the mesa. At this time, chimney pressurization was again initiated in order to maintain pressures necessary to drive gas from the chimney to the mesa. The pressurization continued through swing shift, was shut down during grave and started again on the following day shift. Mesa air sampling was continued on 27 January in an

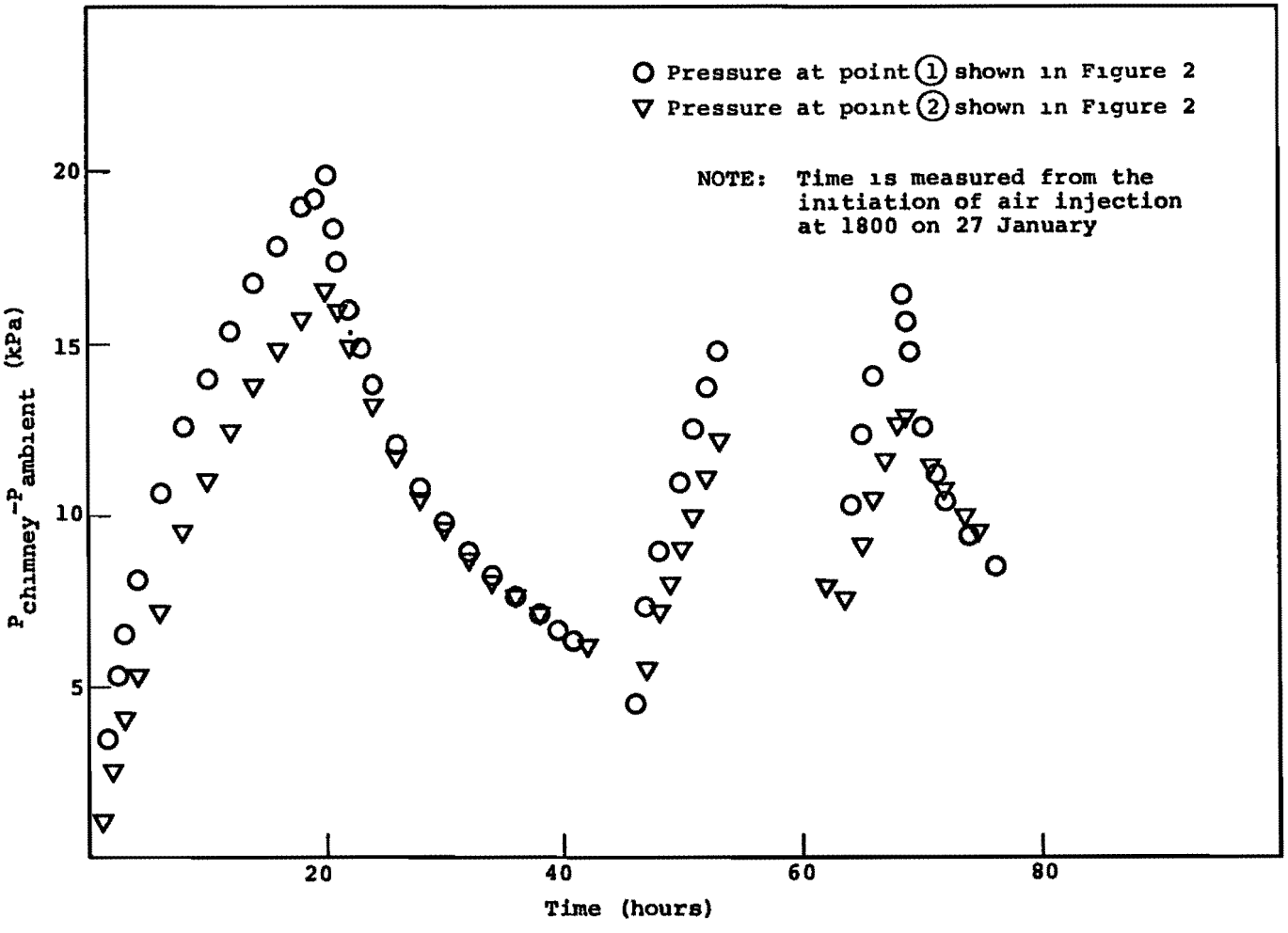

Figure 11 - Measured Dining Car chimney pressure history during the 24 January tracer-gas pressurization test.

Table 1

Results of gas sampling on mesa during the 24 January test

Date	Time	Maximum concentration of Freon 13B1 detected on mesa	Remarks
24	1800	None	Start of air injection into chimney. Freon 13B1 was injected at a concentration of $\sim 10^{-3}$ for a 30 minute period beginning at 1800 hours
25	0030		Tracer arrived at top of chimney at concentration $\sim 10^{-10}$
	0800		
	0900		
	1000		
	1100		
	1200		
	1300		
	1400		
	1500		
	1600	None	
26	0900	4×10^{-11}	
	1400	8×10^{-11}	
27	0800	6×10^{-11}	
	1000	17×10^{-11}	
	1200	4×10^{-11}	
	1400	6×10^{-11}	Freon 13B1 concentration at top of chimney $\sim 10^{-3} \leftrightarrow 10^{-4}$ at this time

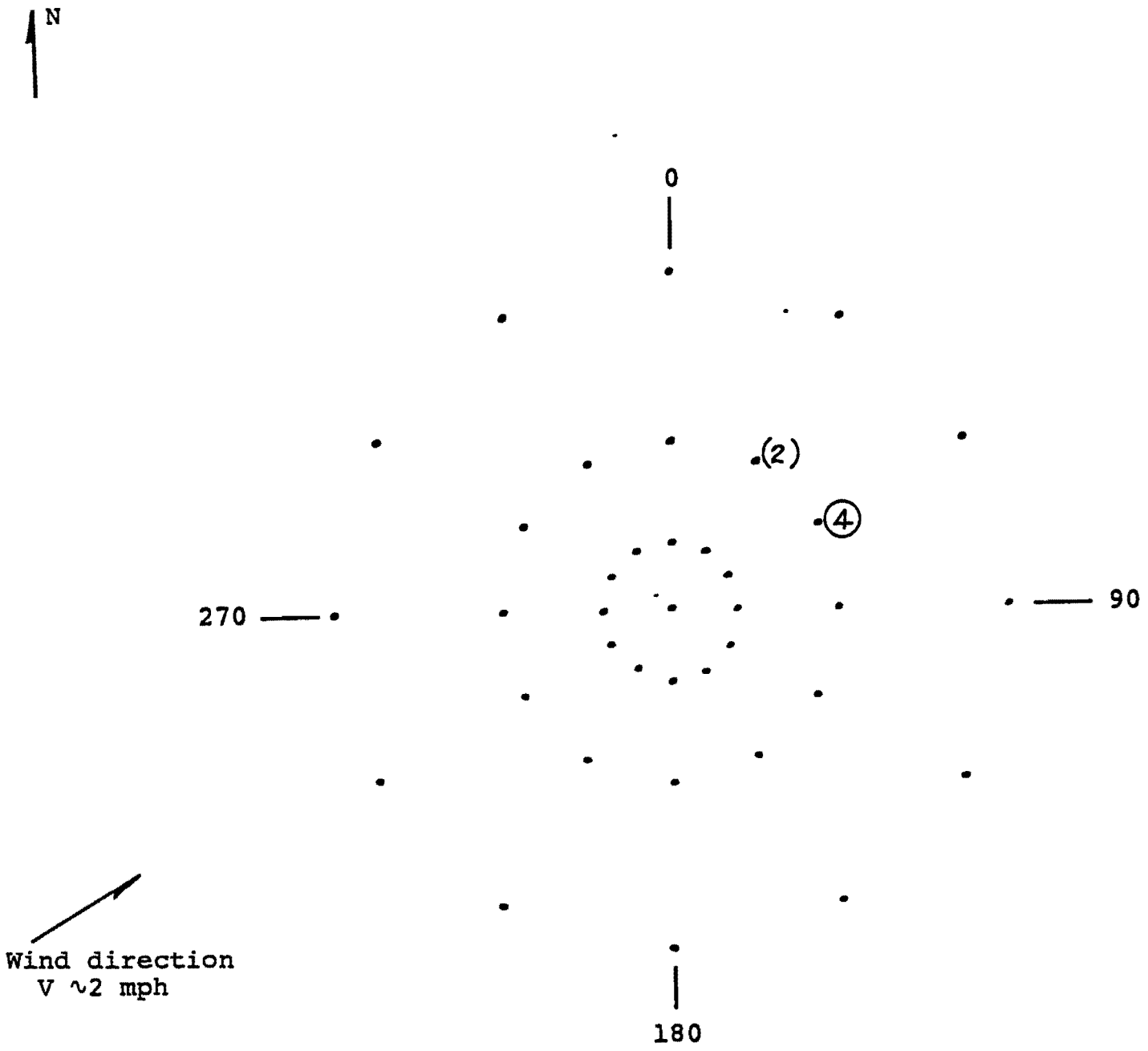

NOTE: Air samples were collected at all positions shown. Numbers indicate Freon 13B1 concentration (x 10^{-11}). These positions correspond to those defined in Figure 5. The B and C units refer to the two gas chromatographs used to analyze the air samples.

( ) = B Unit

◯ = C Unit

Figure 12 - Results of analysis of air samples collected on the mesa at 0900 on 26 January.

attempt to locate the source of seepage. A summary of these measurements is given in Appendix 1. Because the winds were extremely variable throughout the test, it was impossible to determine the exact position of gas seepage. USGS geologists examined the mesa surface at this time for any anamolous geologic formations. They identified a fracture pattern running in a northeasterly direction across the sampling grid shown in Figure 5. The position of this fracture region corresponds reasonably well with the positions at which Freon 13B1 was found on the mesa during the 1000 sweep shown in Figure 13. Mr. Joe LaComb of DNA and Mr. Dave Hoover of USGS indicated this fractured layer probably intersects the uncased U12E18 PS #1 hole leading to the Dining Car chimney. Results of this test, which was intended to determine if gas can flow from the chimney through the paintbrush and caprock material to the mesa, are therefore inconclusive.

One objective of this test was to measure gas communication between the Dining Car chimney and the tunnel complex. Unfortunately, the manifold system shown in Figure 4 was connected to the DN-RE #2 hole using numerous threaded couplings. These threaded joints leaked to such an extent during the 1/2 hour 13B1 injection period that further gas sampling in the tunnel complex was meaningless.

It was found that injection of 1.1×10^5 SCM of air into the Dining Car chimney over a 20 hour period resulted in pressure increases of less than 20 kPa. Gas flow was observed between the injection hole and the top of the chimney. There was no indication of any communication between the injection hole and the working point region of the chimney. Small quantities of tracer gas were detected on the mesa. The flow path for this gas may have been a fractured layer of caprock which intersected the uncased U12E18 PS #1 hole.

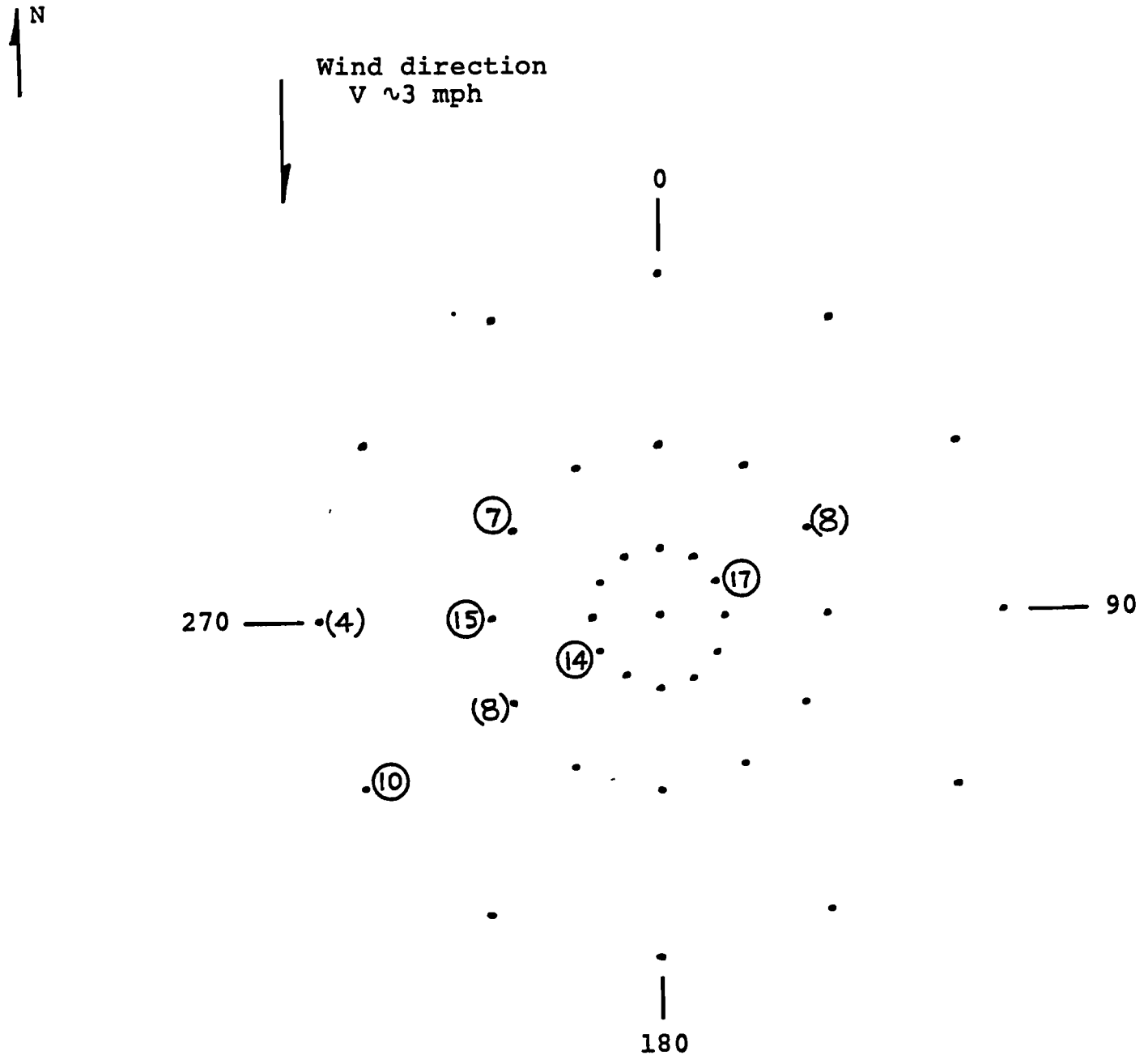

NOTE: Air samples were collected at all positions shown. Numbers indicate Freon 13B1 concentration (x 10^{-11}). These positions correspond to those defined in Figure 5. The B and C units refer to the two gas chromatographs used to analyze the air samples.

( ) = B Unit

◯ = C Unit

Figure 13 - Results of analysis of air samples collected on the mesa at 1000 on 27 January.

4.2.2 1 March Test

The 1 March test was intended to duplicate the 24 January test. In the interim period between these tests, the U12E18 PS #1 hole had been cased and grouted from the mesa to the top of the chimney. All possible leak paths from this hole, through the caprock, to the mesa were thus eliminated. Any tracer gas reaching the mesa during this test must first flow to the top of the chimney and then penetrate 62 m of paintbrush plus 110 m of caprock. A summary comparison of the results obtained during the 24 January and 1 March tests is shown in Table 2.

Pressure histories for these tests are shown in Figures 14 and 15. As shown in Figure 15, the chimney pressure at the beginning of the 1 March test was still 1.7 kPa as a result of the 27 February test. Flow rates were calculated as the flowmeter was inoperable. The air injection rate was determined to be 73.6 SCMM which is about 20 percent lower than the rate determined for the 24 January test. Apparently, either a portion of the uncased length of the DN-RE #2 injection hole had collapsed, material in the injection region of the chimney had shifted, or the material in this region had become more saturated. Because of the lower flow rate, the pressurization period was extended to about 26 hours in order to ensure attaining chimney pressures equivalent to those obtained during the 24 January test. A volume of $\sim 1.1 \times 10^5$ SCM of air was injected during this period. Discontinuities seen in the pressure readings shown in Figure 15 resulted because the 1.25 cm line running from the injection manifold to the end of the casing in the DN-RE #2 hole slowly filled with water throughout the entire test. When indicated pressures became noticeably high, the line would be blown free of water. Absence of the water resulted in a sudden drop in the recorded pressure. If this is taken into account, the pressure rise and decay curves for

Table 2

Comparison of results of Dining Car chimney pressurization tests conducted on 24 January and 1 March

	24 January 1977	2 March 1977
Air volume injected	$\sim 1.1 \times 10^5$ m^3	$\sim 1.1 \times 10^5$ m^3
Duration of injection	20 hours	26 hours
Tracer gas concentration during injection	$\sim 10^{-3}$ 13B1 for <1 hour	$\sim 10^{-4}$ SF_6 for 10 hours
Sensitivity for measuring tracer gas	$\sim 10^{-11}$	$\sim 10^{-12}$
Pressure maximum at top of chimney	16.2 KPa	17.5 KPa
Pressure maximum in inclined hole	19.7 KPa	20.4 KPa
Tracer arrival at top of chimney	6.5 hours	6 hours
Tracer concentration at top of chimney	$10^{-4} \leftrightarrow 10^{-5}$ (@ $\sim$96 hours)	$10^{-4} \leftrightarrow 10^{-5}$ (@ $\sim$72 hours)
Tracer arrival on mesa	24-39 hours	None* (sampling terminated after 44 hours)
Tracer in tunnel complex at completion of pressurization	---	None

*The U12E.18 PS #1 hole through the caprock was cased and grouted for this test. In the 24 January 1977 test, this hole was uncased, but did have a 27.4 m collar at the top. It is anticipated that the 13B1 found on the mesa during the 24 January 1977 test escaped from this ungrouted hole, somewhere between the 27 m depth and the bottom of the caprock located at 110 m, passed through fractures in the caprock finally escaping to the surface.

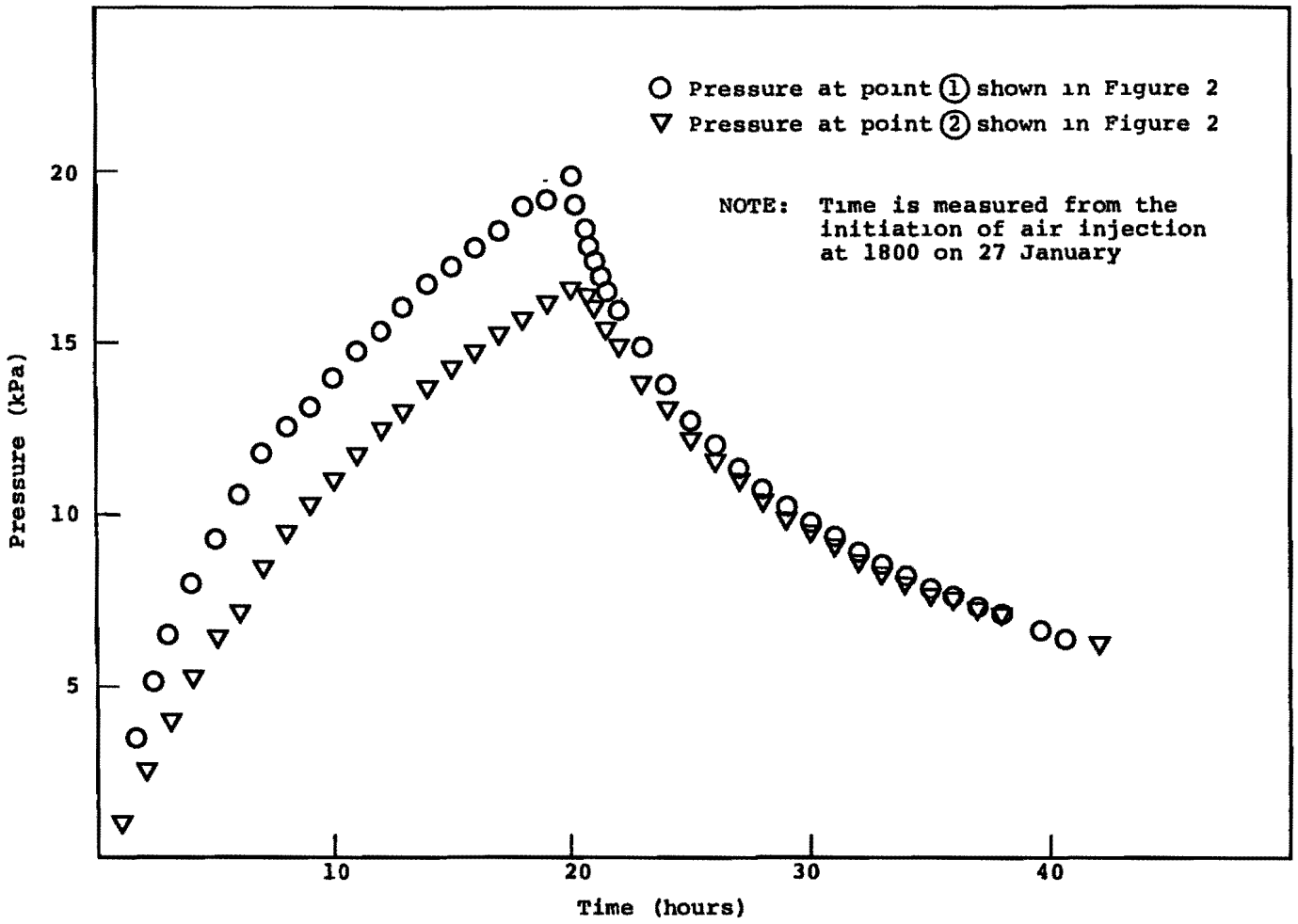

Figure 14 - Pressure history during the first pressurization period for the 24 January test.

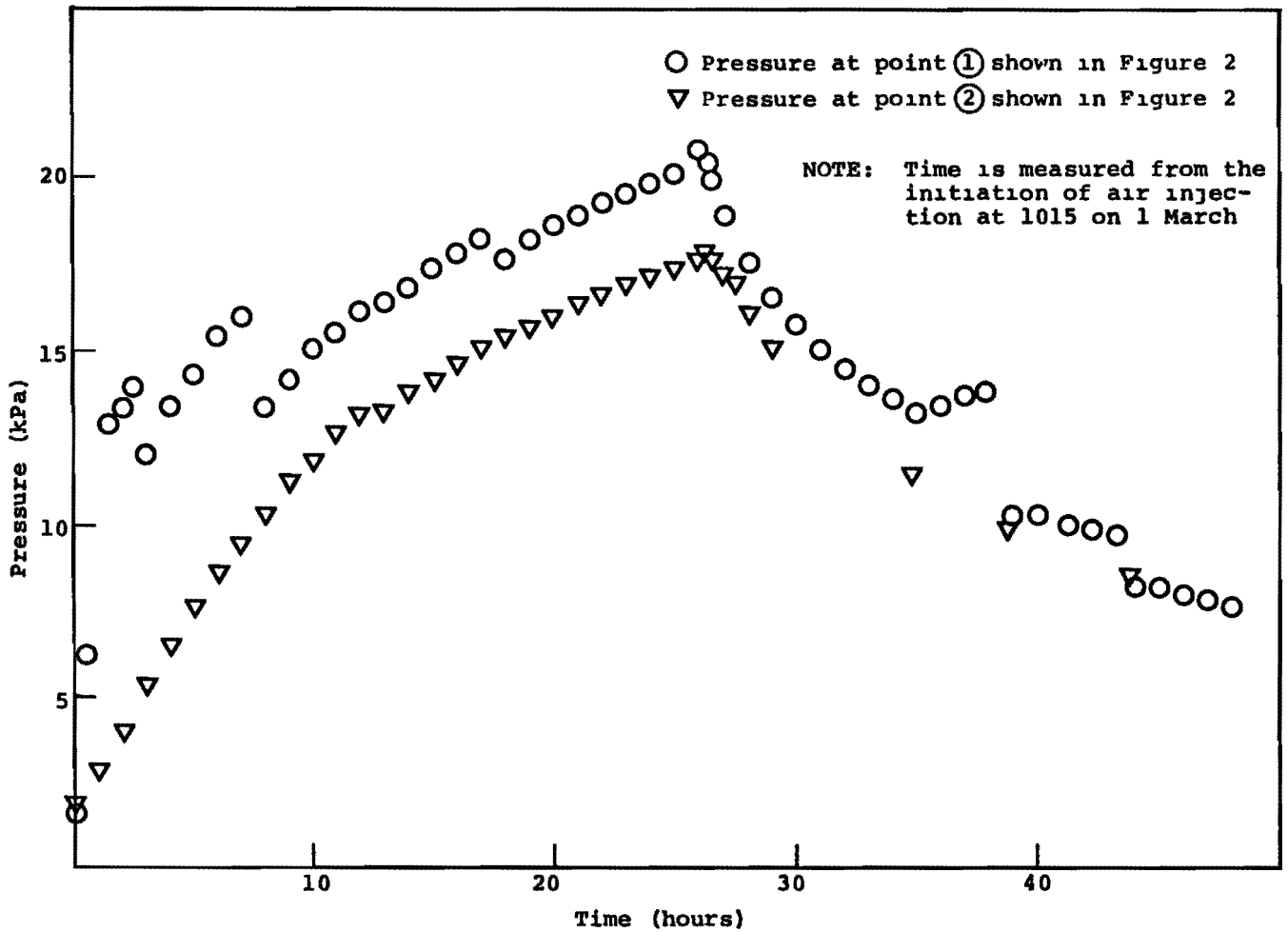

Figure 15 - Pressure history during the 1 March tracer-gas pressurization test.

the 1 March test are seen to be very similar to those obtained during the 24 January test.

Sulphur hexafluoride (SF_6) was used as the tracer gas for the 1 March test. This same gas was used for the 27 February Hybla Gold simulation test. During that test, tracer gas failed to migrate to the top of the chimney. SF_6 injection occurred over a ten hour period at the rate shown in Figure 16. This rate corresponds to an average injection concentration of $\sim 10^{-4}$ parts SF_6 per part air.

Results of the mesa air sampling conducted during this test are summarized in Table 3. A low level concentration of SF_6 was detected at the top of the chimney approximately 6 hours after onset of pressurization. During the 27 January test, 6 1/2 hours were required for Freon 13B1 to reach the chimney top. The seemingly early arrival occurs because 8.5×10^3 m^3 of air containing SF_6 had previously been injected into the chimney during the 27 February test. Gas samples collected on the mesa during the 44 hour period beginning at 1000 on 1 March showed no evidence of SF_6. During the 27 January test, Freon 13B1 reached the mesa sometime within a period of 22 to 39 hours following the onset of pressurization. By 44 hours, 13B1 was readily detectable over at least a third of the sampling grid. As no SF_6 could be detected on the mesa after this 44 hour period, sampling was discontinued.

A 60 percent snow cover existed on the mesa during the 24 January test as compared to a 40 percent cover during this test. Winds were light and variable during both tests. The SF_6 injection concentration was almost an order of magnitude lower than the concentration obtained when injecting 13B1. However, the tracer gas detection equipment is an order of magnitude more sensitive to SF_6 than to 13B1. In terms of sensitivity and ability to detect tracer gas on the mesa, the two tests were equivalent.

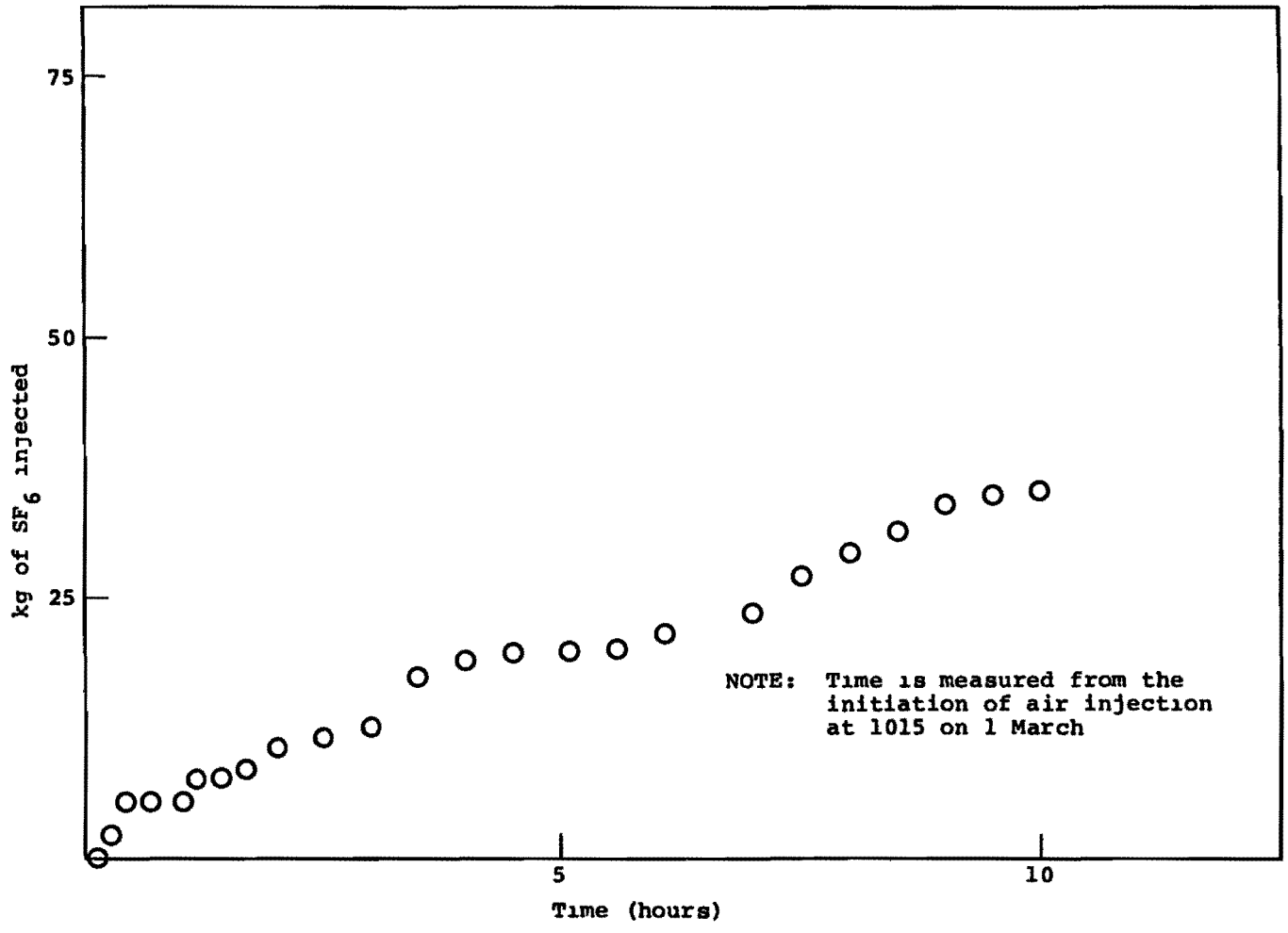

Figure 16 - SF_6 injection rate during the 1 March Dining Car chimney pressurization test.

Table 3

Results of gas sampling on mesa during the 1 March test

Date	Time	Maximum concentration of SF_6 detected on mesa	Remarks
1	1015	None	Start of air injection. SF_6 was injected for 10 hours at a concentration of $\sim 10^{-4}$ parts SF_6 per part air
	1615		Tracer arrival at top of chimney at $\sim 10^{-11}$ concentration
2	1000		
	1400		
	1700		
	2100		
3	0100		
	0600	None	
4	1000		Tracer concentration at top of chimney $\sim 10^{-4}$ to 10^{-5}

SF_6 began leaking from the top of the drill stem on the U12E18 PS #1 hole 20 hours after it was first detected at the top of the chimney. The leak occurred through threaded joints near the top of the pipe. The joints on the pipe stem itself were immediately welded, thus greatly reducing the leak rate. However, there remained some seepage from the threaded joints to the valves leading to the manometer lines and gas sample pump. These joints could not be welded, sealed or bypassed. Although these remaining leaks were small, they could not be permitted as any SF_6 leaking onto the mesa could possibly compromise the bulk of the mesa data. A bottle of nitrogen was therefore attached to the topmost connection of the drill stem. Nitrogen was allowed to flow into the U12E18 PS #1 hole at a pressure slightly ($\leq$ 1/2 in. of water) greater than the chimney pressure, thus preventing any SF_6 leakage. This flow was continued until termination of air sampling on the mesa 18 hours later. A total of 11 m^3 of nitrogen was injected.

Previous attempts had been made to determine communication between the Dining Car chimney and tunnel complex. During these tests, tracer gas had leaked from the injection manifold. Subsequently, tracer gas was found in the tunnel complex, however, there was no indication this gas came from the chimney. By 1 March, there existed only a trace of SF_6 in the tunnel complex as a result of the 27 February test. During the 1 March test, no SF_6 escaped from the injection manifold. Communication between the chimney and tunnel complex could therefore be evaluated unambiguously. Gas samples collected at the tunnel sampling stations shown in Figures 3 and 6 at the end of the 26 hour pressurization period showed no evidence of SF_6.

In terms of injected air volumes and attained chimney pressures, the 1 March test closely represented the 27 January test. During this later test, there was no indication of gas flow from the Dining Car chimney to the mesa surface or tunnel complex.

5. DETERMINATION OF MATERIAL PROPERTIES

The tracer gas pressurization technique may be used to determine the properties of the chimney material and its surroundings. Quantitative evaluation of the distribution of acceptable void volume and effectively permeability can be determined. The extent of fracturing within the chimney material can also be qualitatively evaluated. In addition, communication through the chimney and through the surrounding media can be directly measured by monitoring tracer gas arrival.

Media properties are determined as follows. First the chimney geometry and surrounding geology must be defined. Preferably, the surrounding media properties are also known. The chimney is then tested to a moderate pressure by injecting air containing a tracer gas. During this test, the gas injection rate, source pressure and tracer gas concentration are carefully measured. Resulting pressures and tracer gas concentration histories are then measured at points of interest. A two-dimensional finite element, time-dependent code named GASFLOW is then used in an iterative manner to aid in determining void volumes and permeabilities consistent with the measured data. Specifically, a set of material properties is selected. A calculation is then made using this set of material properties and the known injection rates. Calculated pressures are then compared with the experimentally measured pressures taken during both the pressurization and decay periods. Various sets of material properties are selected until the calculated and measured pressures agree. Once agreement is attained, the iteration is complete, and those material properties are assumed to be correct for the assumed geometry.

Brief descriptions of the analytical/numerical technique and geometrical approximations are given in Section 5.1. Calculational results including the properties of the chimney

and surrounding media are presented in the next section. Finally, the sensitivity of these results to the selected distribution of effective permeability and accessible void volume are discussed in Section 5.3.

5.1 ANALYTICAL/NUMERICAL TECHNIQUE

The analysis assumes simple Darcy flow. Thus, the area average fluid velocity $\bar{q}$ is proportional to the gradient in pressure, p, giving

$$\bar{q} = - \frac{k}{\mu} \nabla p \tag{2}$$

where k and μ are the permeability and fluid viscosity, respectively. The corresponding fluid particle velocity (i.e., tracer particle velocity) is just

$$\bar{v} \equiv \frac{\bar{q}}{\phi} \tag{3}$$

where ϕ is a porosity. Equation (2) combined with the mass conservation equation and equation of state

$$\phi \frac{\partial \rho}{\partial t} + \nabla \cdot (\rho \bar{q}) = w \tag{4}$$

$$p = c\rho^{\gamma} \tag{5}$$

where ρ, γ and c represent density, ratio of specific heats and a constant, respectively, yield the defining equation for compressible flow in the porous media.

$$\phi \frac{\partial}{\partial t} \left(p^{\frac{1}{\gamma}} \right) = \nabla \cdot \left\{ \frac{kP}{\mu} \gamma \nabla \left(p^{\frac{1}{\gamma}} \right) \right\} + w c^{\frac{1}{\gamma}} \tag{6}$$

The terms on the far right hand side of Equation (4) and (6) simply represent a source within the media. Solutions to

Equation (6) in two-dimensions (e.g., either axisymmetric or Cartesian coordinates) are obtained using the finite element GASFLOW code. The GASFLOW code is an extension of the finite element heat conduction code written by Wilson.[3] Results presented here assume isothermal flow (with $\gamma = 1$) and an isotropic media having a scalar permeability.

During the tracer-gas pressurization tests, air flow is measured through the highly saturated possibly fractured porous materials. It is therefore implicit in the use of Equation (6) that k and ϕ represent the effective permeability and accessible void fraction, respectively. They do not represent a dry permeability or total porosity. If the grain and in situ densities are determined (from core samples, etc.), then these latter quantities can be inferred from knowledge of the effective permeability and accessible void fraction. Given these properties, the flow of steam plus a non-condensible gas into the Dining Car chimney can be analyzed.

Analytically, the tracer gas motion is determined by following tracer particles, having a velocity defined by Equation (3), through the numerical grid. The tracer particle motion determined by the calculation can then be compared to the tracer gas arrival time determined by sampling from various positions in the chimney. Given a uniformly porous material, the calculated and measured tracer particle arrival times agree provided the calculated and measured pressure histories agree. Furthermore, the tracer gas concentration upon arrival should be essentially equivalent to the injection concentration. Experimentally measured early tracer gas arrivals at low concentration levels imply a fractured medium. When fractured, some tracer gas may rapidly flow through a crack to the sampling region. The tracer gas concentration at this region is much lower than the concentration at the injection region since only a portion of the tracer gas flows in this manner. A comparison

of the measured and calculated tracer gas arrival times and concentrations therefore provides a qualitative indication of the amount of fracturing within the material.

The Dining Car chimney geometry shown in Figures 1 and 2 can be well represented by the numerical grid shown in Figure 17. In addition, the layering of the surrounding media is easily represented on this grid. The only feature not well represented using this axisymmetric geometry is the source used for air injection. The presence of the ∿10 cm dia 17 m long cylindrical source described in Figure 2 truly makes the problem three-dimensional. For analysis purposes, the source is assumed spherical and positioned on the chimney centerline. Its flow rate is taken equivalent to that of the cylindrical source. The resulting source pressure is that required to provide this flow and is generally not equivalent to that of the cylindrical source. Because the permeability of the chimney material is high, the chimney response depends strongly on the air injection rate, but is independent of the source geometry except in the immediate vicinity of the source. As a result, accurate pressure comparisons should not be expected at the injection point during pressurization periods. However, during decay periods, which usually last many hours, accurate comparisons can be made at the source position between calculated and measured pressures since all geometrical effects introduced by the modeling of the cylindrical source have long since vanished.

5.2 CALCULATED MATERIAL PROPERTIES

Selection of material properties requires interpretation of detailed comparisons between calculated and experimental pressure data. The 24 January data, shown in Figures 11 and 14, were selected for this study because of their completeness and consistency. From these data, it is desired to determine

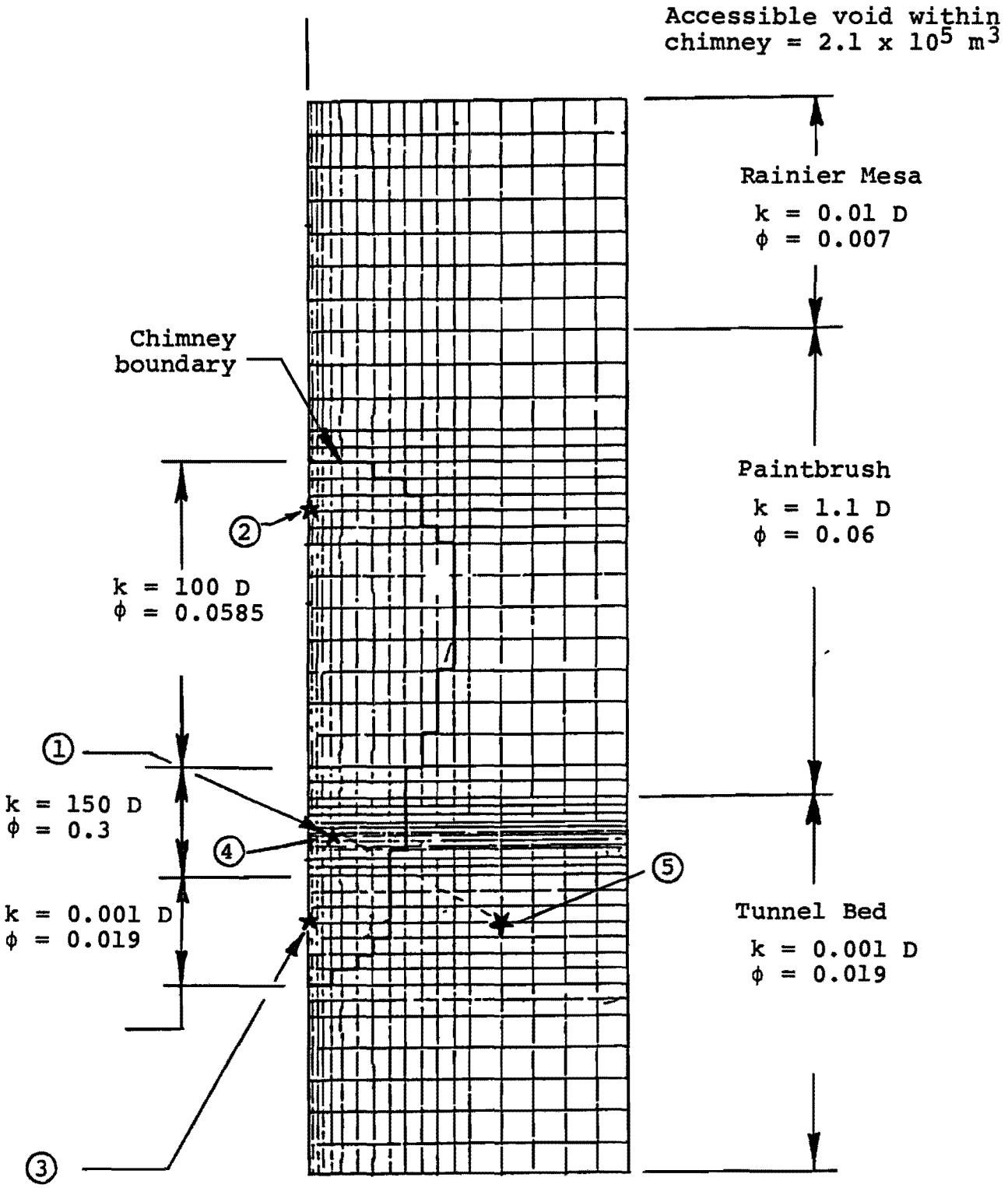

Figure 17 - Calculational grid for Dining Car chimney showing distribution of material properties.

the distribution of effective permeability and accessible void volume within the chimney, and the effective permeability and accessible void content of the paintbrush and tunnel bed material surrounding the chimney. This sizable number of material property values must be determined from data taken from three points within the chimney, one of which failed to show any pressure change during the first pressurization and decay cycle.

Before presenting the detailed results, it may be helpful to discuss the relationship between the various material properties and the characteristics of the data shown in Figure 14. The average rate of pressure increase during the beginning of the pressurization period is most sensitive to the total accessible void volume within the chimney. Pressure differences between points ①, ② and ③ within the chimney are primarily a function of the distribution of effective permeability and accessible void volume within the chimney. The curve shapes during the later portion of the pressurization period and throughout the entire decay period are functions of the material properties of the paintbrush and tunnel bed materials surrounding the chimney. A solution which reproduces the experimental data must therefore incorporate correct material properties for all these regions. All solutions presented here assume the chimney geometry, taken as shown in Figure 1 and 2, can be adequately represented by the grid shown in Figure 17.

Because the source geometry cannot be modeled exactly, pressures calculated for point ① shown in Figure 2 may not reproduce experimental values during the pressurization period. However, good agreement should be obtained between measured and calculated pressures at other points within the chimney during pressurization periods. During the decay period, the chimney geometry is modeled correctly and calculated and measured pressures should agree everywhere. Because there was no communication between points ① and ③, only an upper bound can be determined for the value of effective permeability in

this region. For all practical purposes, the Rainier Mesa member is impermeable and its properties cannot be determined from this test. An additional constraint in selecting material properties is the requirement for conservation of accessible void volume. The total accessible void volume within the chimney must be the sum of the cavity volume plus the accessible void volume of the material which collapsed to form the chimney.

A "best estimate" of the material properties of the Dining Car chimney and surrounding media are shown in Figure 17. This chimney has an accessible void volume of 2.1 x 10^5 m^3. As shown in Figures 18 and 19, calculated pressures reproduce the measurements throughout the complete 80 hour test period. Calculated pressure histories for various points within the chimney are shown in Figure 20. The pressure distribution after 76.5 hours is shown in Figure 21. At the end of the first pressurization period, it is seen that significant pressure differences do occur within the chimney. However, the working point pressure remains constant. During the decay period, pressures in the region between points ① and ③ equilibrate. By 76.5 hours, there exist measurable pressures in the paintbrush material at large distances away from the chimney. At this time, a slight pressure is calculated for point ③. Because there is no data for this point at this time, it cannot be determined if this pressure rise is real or if too large a value has been used for the effective permeability of the lower chimney material.

In terms of material properties, the chimney may effectively be divided into three regions. In the upper region, the material has an effective permeability of 100 darcies with an accessible void fraction of 0.0585 which is similar to that of the surrounding paintbrush material. The middle layer of the chimney has an even higher effective permeability of about 150 darcies and a very high accessible void fraction of 0.3.

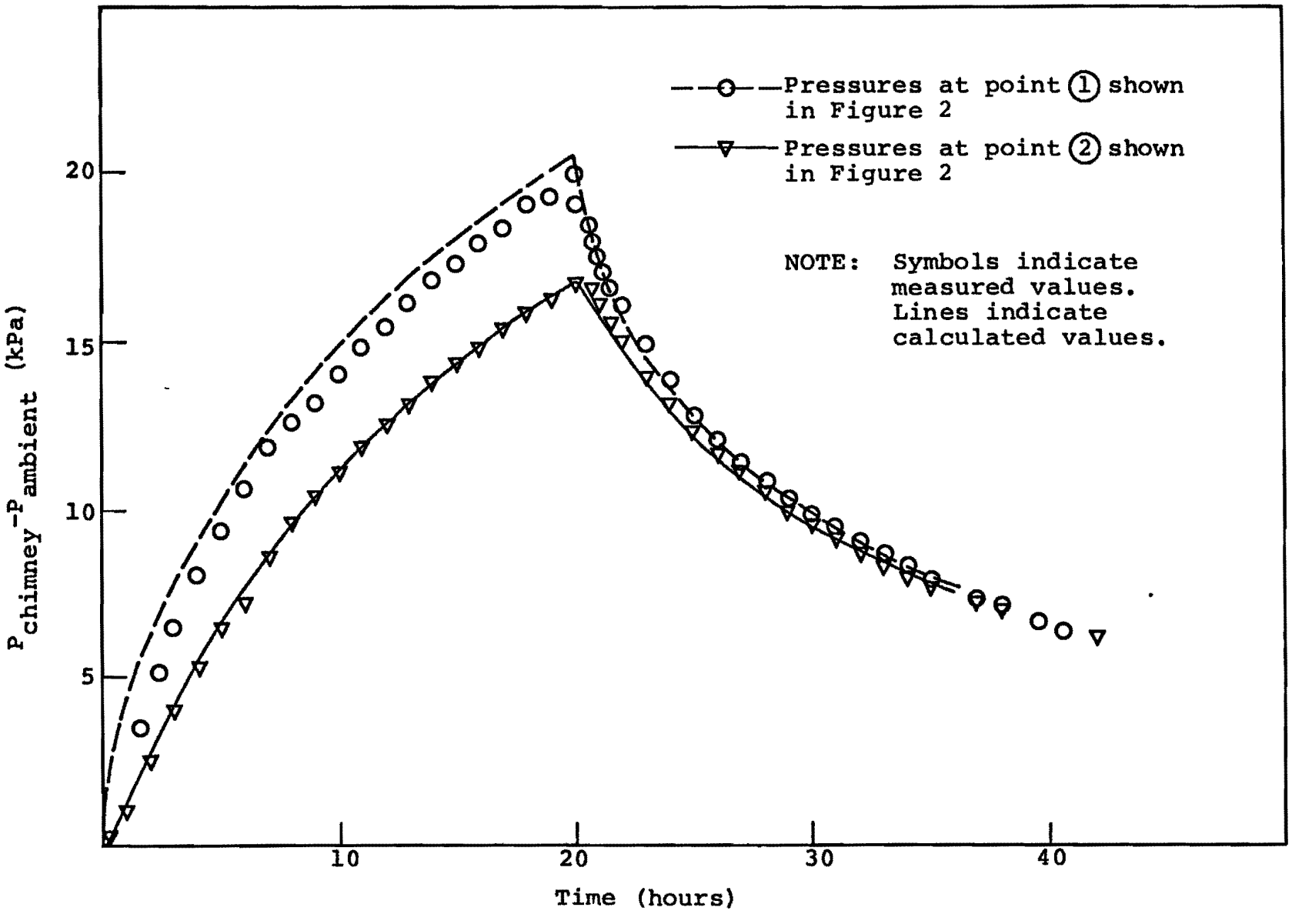

Figure 18 - Comparison of calculated and measured chimney pressure histories using material properties shown in Figure 17.

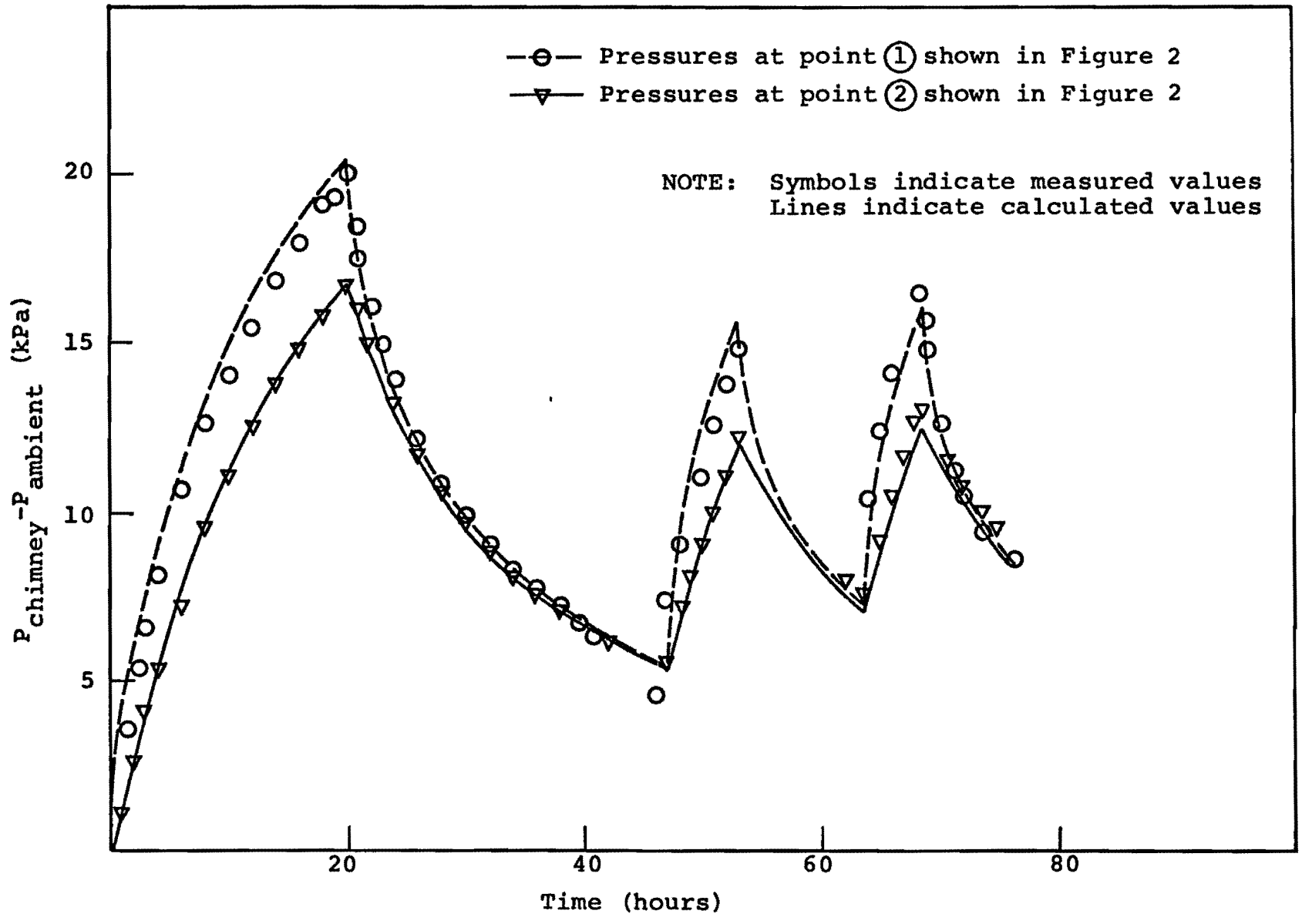

Figure 19 - Comparison of calculated and measured pressures for 27 January test using material properties shown in Figure 17.

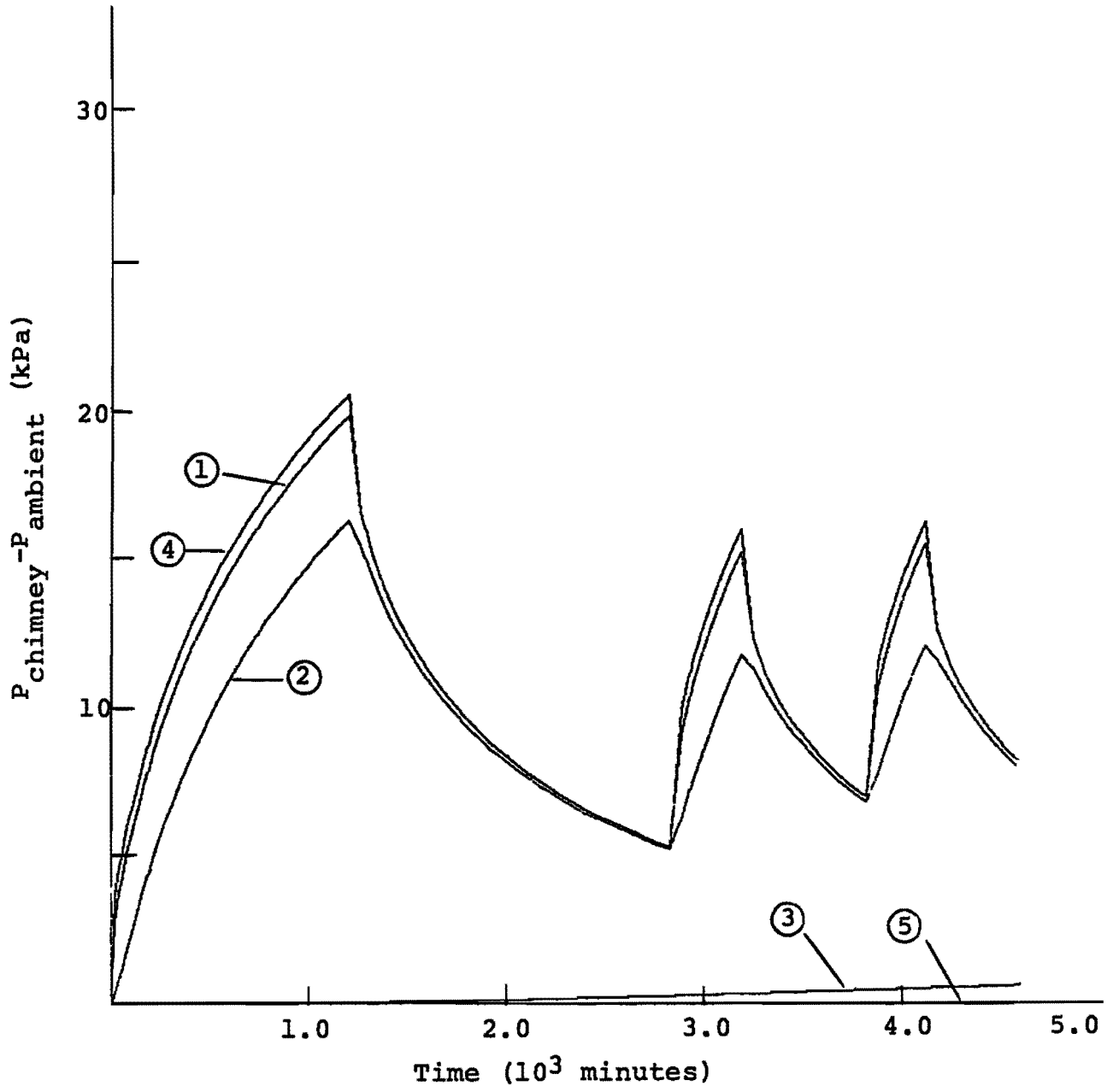

Figure 20 - Numerical plot of pressure vs time history at points (1) through (5) shown in Figure 17.

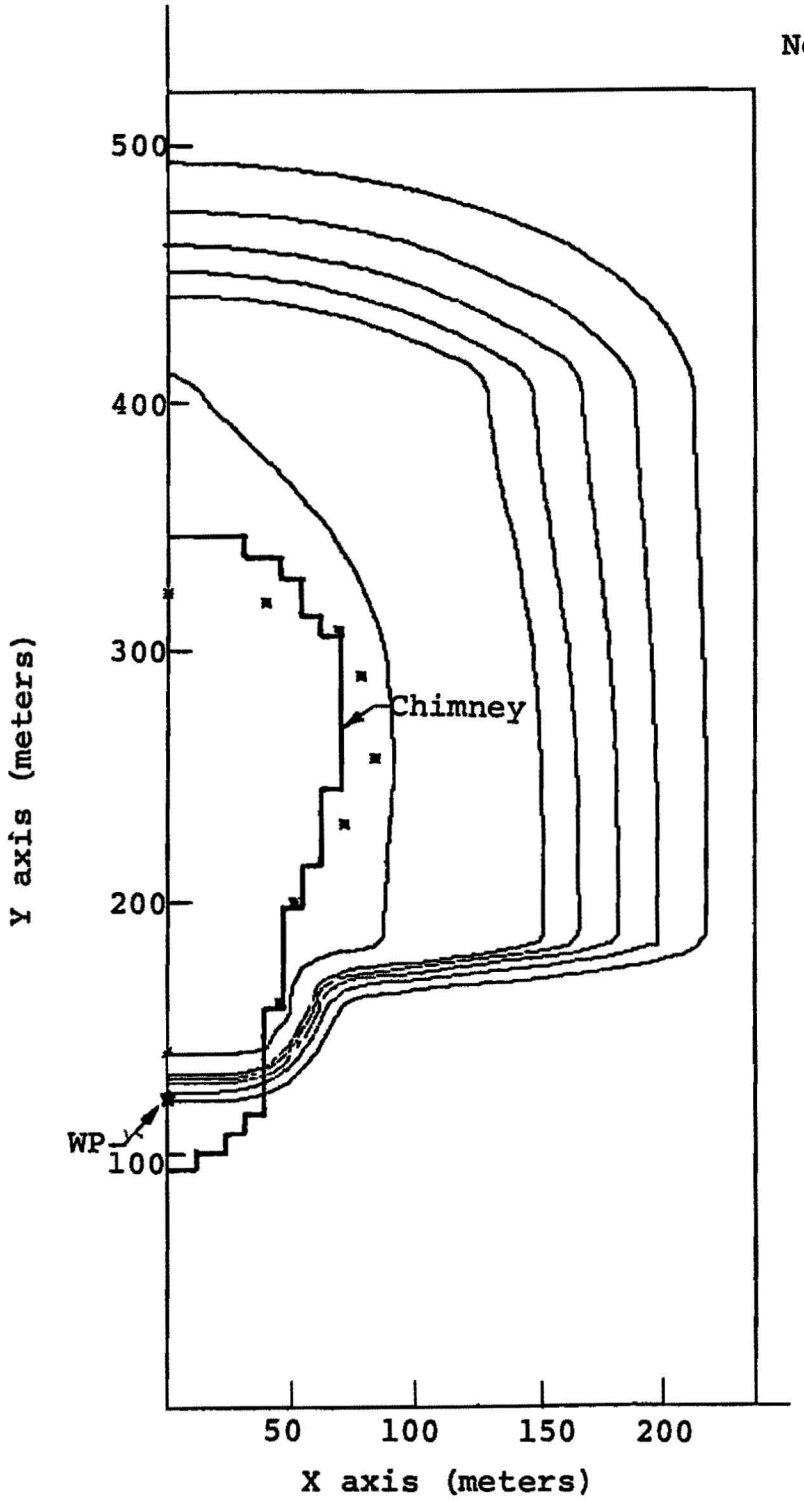

Note: The contours shown represent constant pressure values measured with respect to the ambient pressure. Beginning with the outermost contour, these lines represent pressures of 0.68, 1.36, 2.04, 2.72, 3.40 and 6.80 kPa, respectively.

Figure 21 - Numerical plot showing pressures and tracer positions after 76.5 hours.

Material properties in the lower portion of the chimney are assumed the same as the tunnel bed tuff. The effective permeability of this material must be less than 1 millidarcy. Its accessible void volume cannot be determined because there was no recordable pressure change at point ③. The paintbrush material was found to have an effective permeability of 1.1 darcy and an accessible void fraction of 0.06.

Figure 22 shows the calculated tracer gas migration during the test period. After 76.5 hours, the tracer-gas cloud is just approaching the upper chimney boundary. As shown in Table 2, the SF_6 concentration at the top of the chimney is approaching the injection concentration after 72 hours. Low concentrations of tracer gas were found at the top of the chimney approximately 6 hours after pressurization started. The observed early arrival at point ② of low concentrations of tracer gas indicate the material between points ① and ② is significantly fractured.

The distribution of material properties implied by this analysis is difficult to explain. The upper portion of the chimney is filled with paintbrush material which is fractured, but which has not significantly bulked. Most of the bulking appears to occur in the middle portion of the chimney filled with zeolitized paintbrush material. Lower regions may be filled with competent tunnel bed material, thus accounting for the apparent low value of effective permeability.

5.3 SENSITIVITY OF RESULTS

Calculated pressures were compared with measured pressures for 32 sets of material property distributions. To provide an indication of the accuracy of the material properties selected in Section 5.2, the results of calculations completed using three different sets of material properties will be presented here. A complete summary of the various sets of material

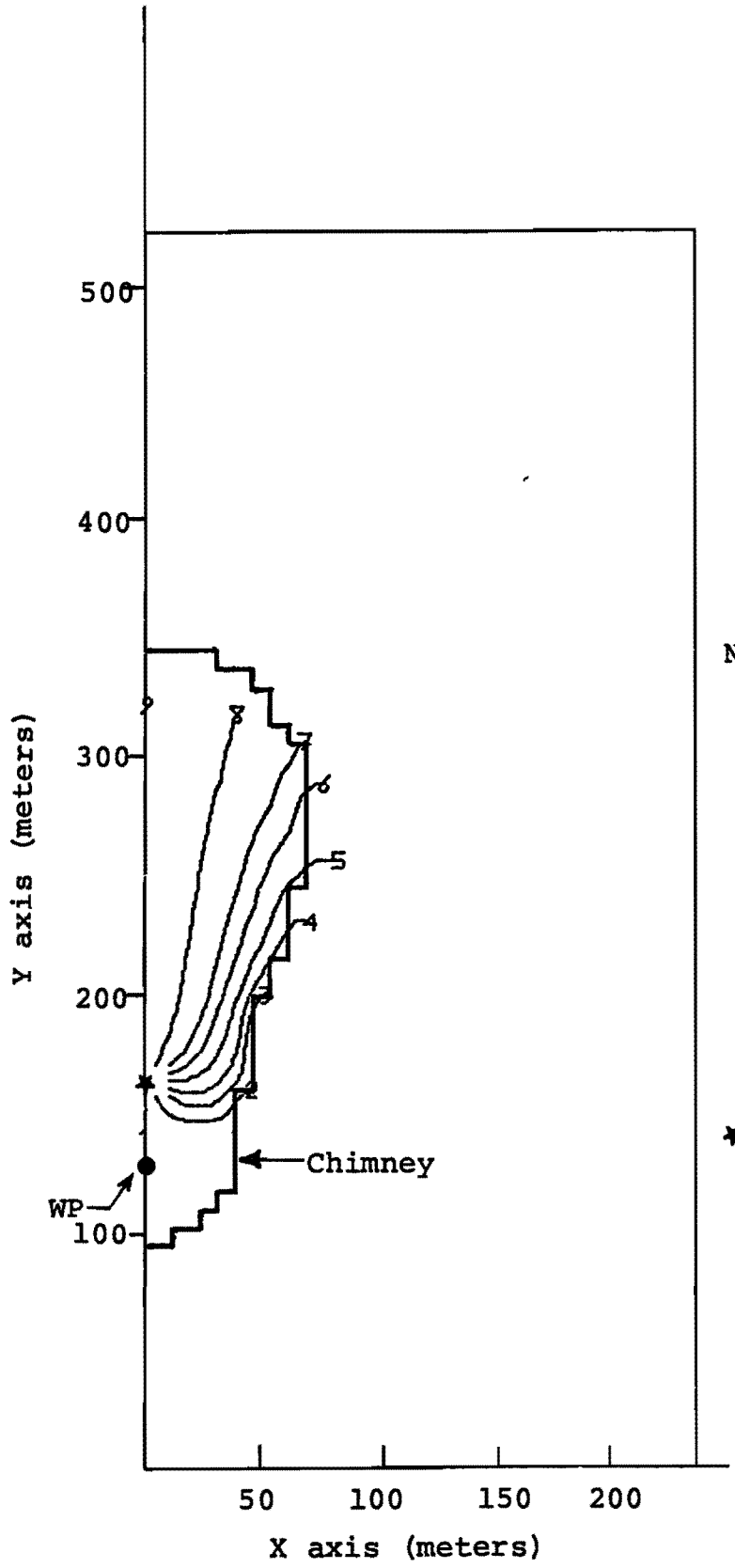

Figure 22 - Numerical plot of tracer gas movement during the 76.5 hour period described in Figure 20.

property distributions is given in Table 4.

A number of calculations were completed assuming the accessible void volume was nearly uniformly distributed throughout the entire chimney. Within this group of calculations, the material property distribution shown in Figure 23 provided the best result. Except for the distribution of accessible void volume within the chimney, these material properties are identical with those given in Figure 17. A comparison of the calculated pressure history with the measured data is shown in Figure 24. Generally, the results are comparable with those shown in Figure 18 except during the pressure decay period. During this period, the calculated time required for the chimney pressure to equilibrate is much shorter ($\sim$6 hours) than the time indicated by the experimental data ($\sim$16 hours). As shown previously, a longer equilibration time is obtained when the middle portion of the chimney has a higher accessible void volume.

Because the chimney is formed by material collapsing into the cavity region, it could realistically be assumed that maximum bulking occurs at the top of the chimney. A possible model would have a small accessible void fraction in the lower regions of the chimney. This accessible void fraction would steadily increase as the top of the chimney is approached. The associated change in effective permeability can be approximated using the Kozeny relation given in Bear.[4] If the chimney interior is taken to fit this description, then the best comparison between calculated and measured results is obtained using the material property values shown in Figure 25. It is seen in Figure 26 that the calculated pressure equilibration rate during the decay period is very short compared to the measured rate. This material property set cannot be considered realistic.

Table 4

Summary of GASFLOW calculations

Group	MATERIAL PROPERTIES: Upper portion of chimney k	Upper portion of chimney φ	Source region k	Source region φ	Lower portion of chimney k	Lower portion of chimney φ	Paintbrush k	Paintbrush φ	Remarks
I*	100	0.09	150	0.09	150	0.09	1.2	0.044	Unsatisfactory
	100	0.06	100	0.06	100	0.06	1.2	0.044	Unsatisfactory
II*	100	0.05	100	0.05	100	0.05	0.7	0.044	Unsatisfactory
	100	0.05	100	0.05	100	0.05	0.7	0.050	Unsatisfactory
	100	0.05	100	0.05	100	0.05	0.8	0.044	Unsatisfactory
	100	0.05	100	0.05	100	0.05	0.9	0.034	Results acceptable at points ① and ② shown on Figure 2. Accessible void fraction in chimney and paintbrush materials unacceptably low.
III*	100	0.1	100	0.2	100	0.2	0.9	0.034	Assume larger accessible void fraction in chimney. Results unacceptable
	150	0.1	100	0.2	100	0.2	0.9	0.034	" " " " "
	150	0.1	100	0.2	100	0.2	0.9	0.024	" " " " "
IV	100	0.1	150	0.3	0.36	0.067	0.9	0.034	Use tunnel bed tuff properties in lower chimney region.
	100	0.1	150	0.3	0.36	0.067	1.0	0.024	" " " " "
	100	0.07	100	0.5	0.36	0.067	1.0	0.024	Results acceptable at points ① and ②. Pressure at point ② unacceptably large. Paintbrush void fraction unacceptably low.
V	500	0.1	500	0.09	0.36	0.067	3.0	0.06	Uniform properties within chimney, results unacceptable
	250	0.1	250	0.09	0.36	0.067	3.0	0.06	" " " " "
	250	0.1	250	0.09	0.36	0.067	1.0	0.06	" " " " "
	100	0.1	100	0.09	0.36	0.067	1.0	0.06	" " " " "
	100	0.1	100	0.09	0.36	0.067	0.9	0.06	Results acceptable at points ① and ②. Pressure at point ③ unacceptably large.
VI	400-80	0.15-0.08	35-10	0.06-0.04	1-0.5	0.02-0.01	1.2	0.06	Linear variation of porosity within chimney with Kozeny permeability distribution.
	1600-320	0.15-0.08	140-40	0.06-0.04	4-2	0.02-0.01	1.2	0.06	" " " " "
	1600-320	0.15-0.08	140-40	0.06-0.04	4-2	0.02-0.01	0.9	0.06	" " " " "
	1600-320	0.15-0.08	140-40	0.06-0.04	4-2	0.02-0.01	0.8	0.06	Results acceptable at points ① and ②. Pressure at point ③ unacceptably large.
VII	100	0.06	150	0.30	0.36	0.067	0.9	0.06	Attempt variations in φ and k within chimney. Results unacceptable.
	100	0.03	100	0.25	0.36	0.067	0.9	0.06	" " " " "
	125	0.06	125	0.3	0.36	0.067	0.9	0.06	" " " " "
VIII					WP and TB properties				
	100	0.0585	150	0.3	0.01	0.019	0.9	0.06	Determine bounds on effective permeability of lower chimney and tunnel bed material
	100	0.0585	150	0.3	0.0001	0.019	0.9	0.06	" " " " "
	100	0.0585	150	0.3	0.001	0.019	1.2	0.06	" " " " "
	100	0.0585	150	0.3	0.001	0.019	1.1	0.06	Figure 18 and 19 (provides best simulation of experimental results)
IX	100	0.1	100	0.084	0.001	0.019	1.1	0.06	Results unacceptable
	100	0.1	150	0.084	0.001	0.019	1.1	0.06	Figure 24 (uniform material properties in chimney)
	1600-320	0.15-0.08	140-40	0.06-0.04	0.001	0.019	1.1	0.06	Figure 26 (linear variation of void volume, Kozeny permeability distribution)
X	90	0.0527	135	0.27	0.001	0.019	0.99	0.054	Figure 27 (sensitivity study)

*These analyses had been completed before the 2 March test. At that time, it was determined there was no communication during the pressurization period between points ① and ③ shown in Figure 2.

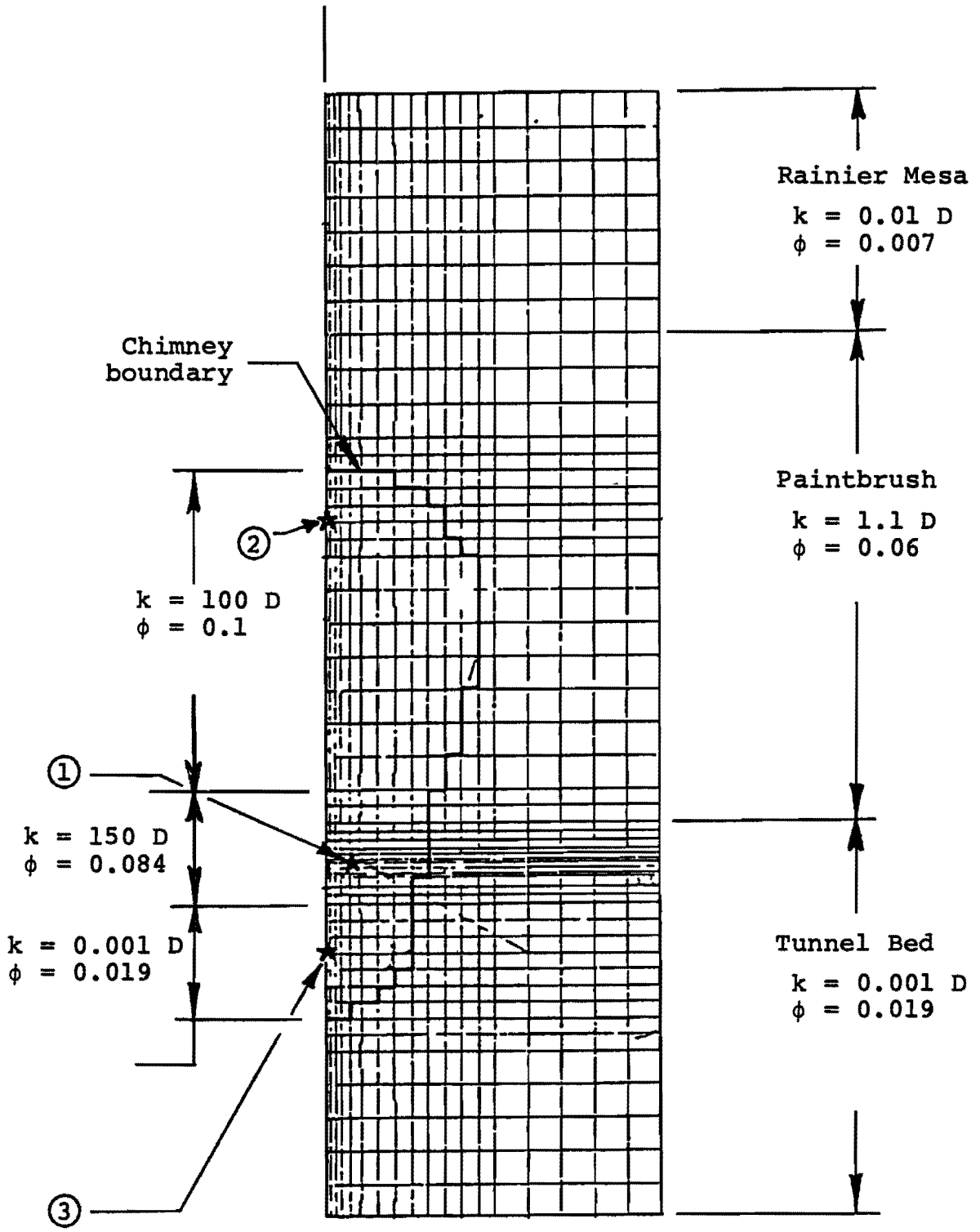

Figure 23 - Material property distribution and calculational grid assuming nearly uniform distribution of accessible void volume in chimney.

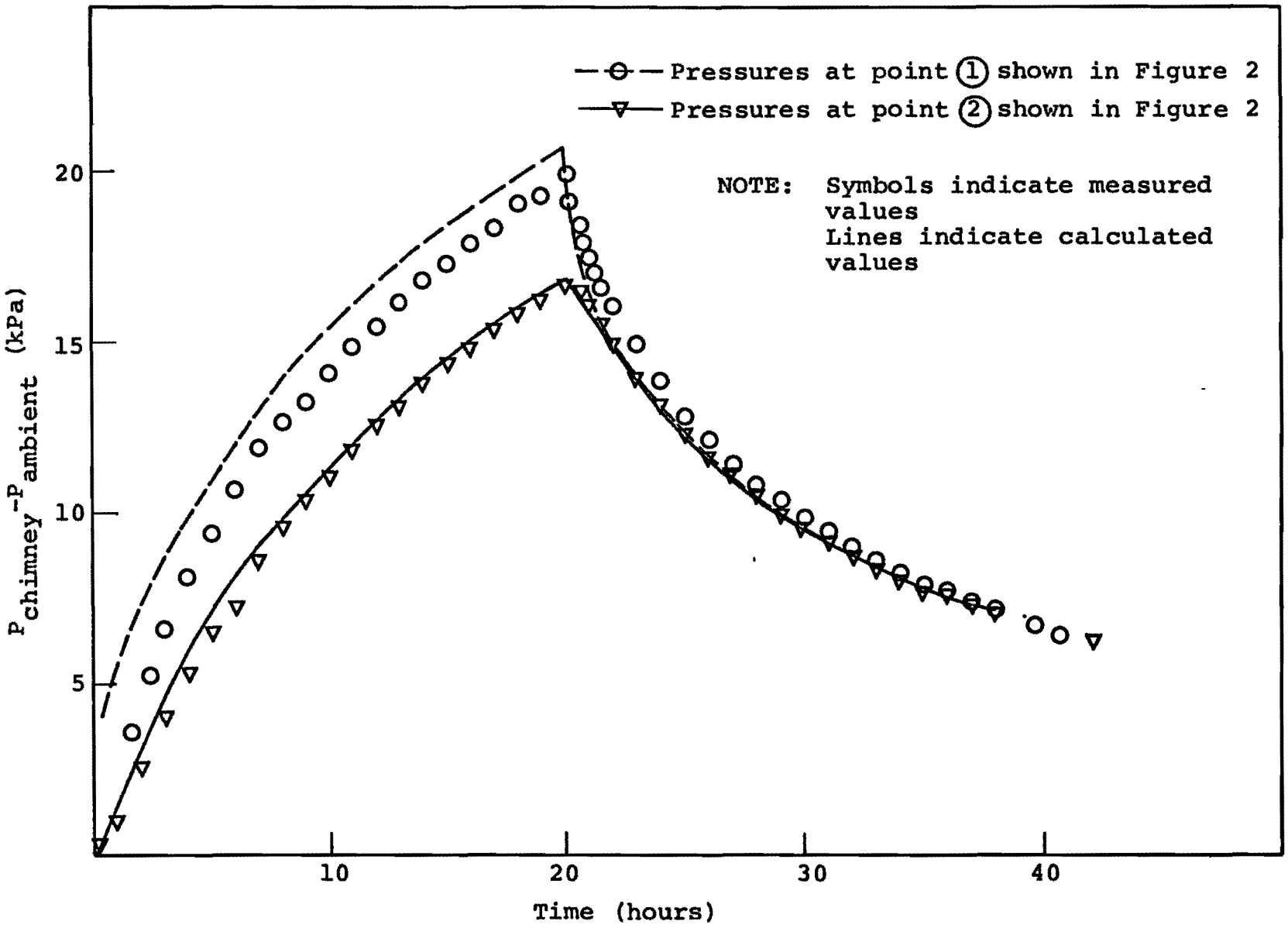

Figure 24 - Comparison of calculated and measured chimney pressure histories using material properties shown in Figure 23.

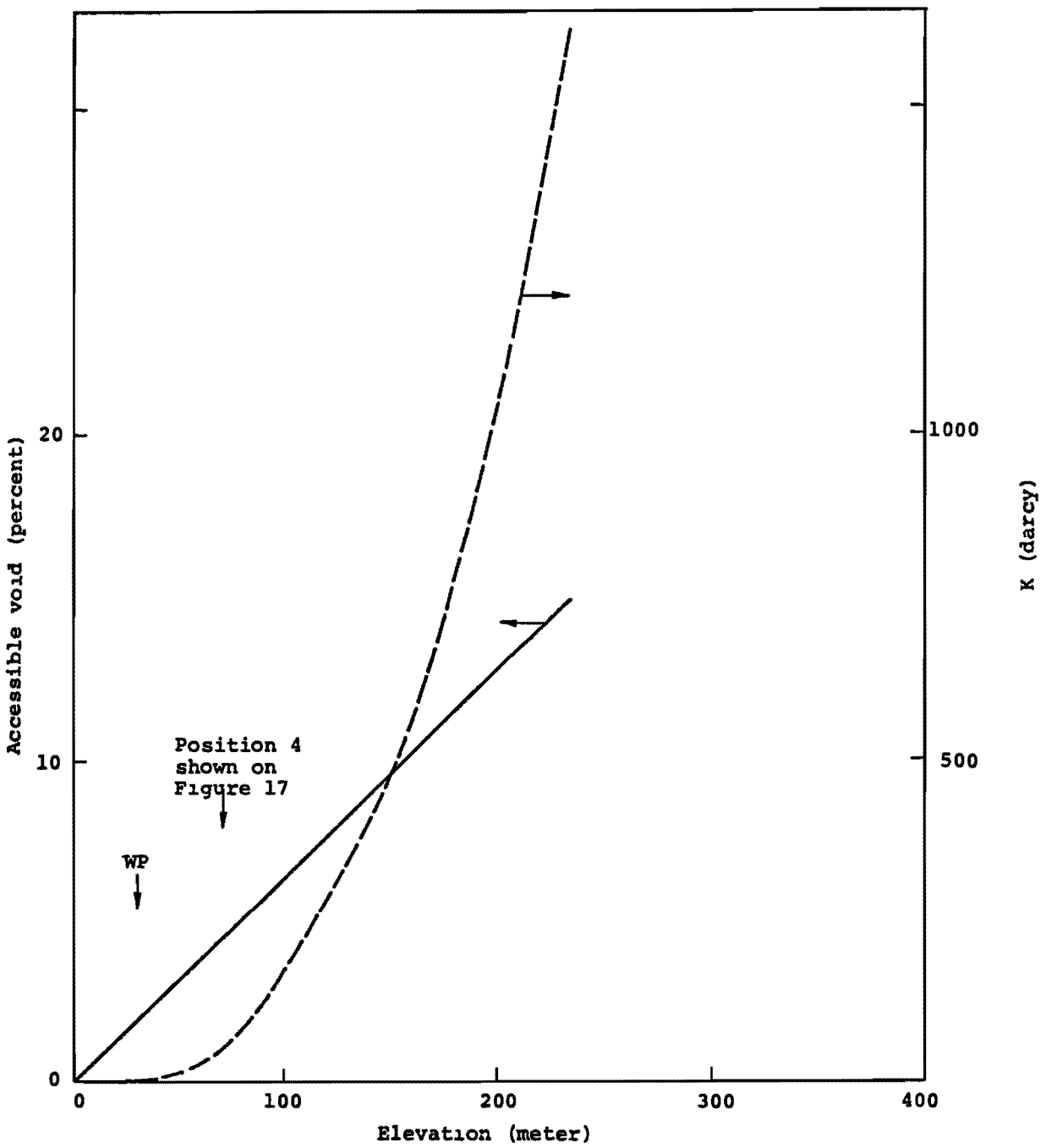

Figure 25 - Distribution of permeability and accessible void volume within the chimney used to obtain the calculated pressures shown in Figure 26.

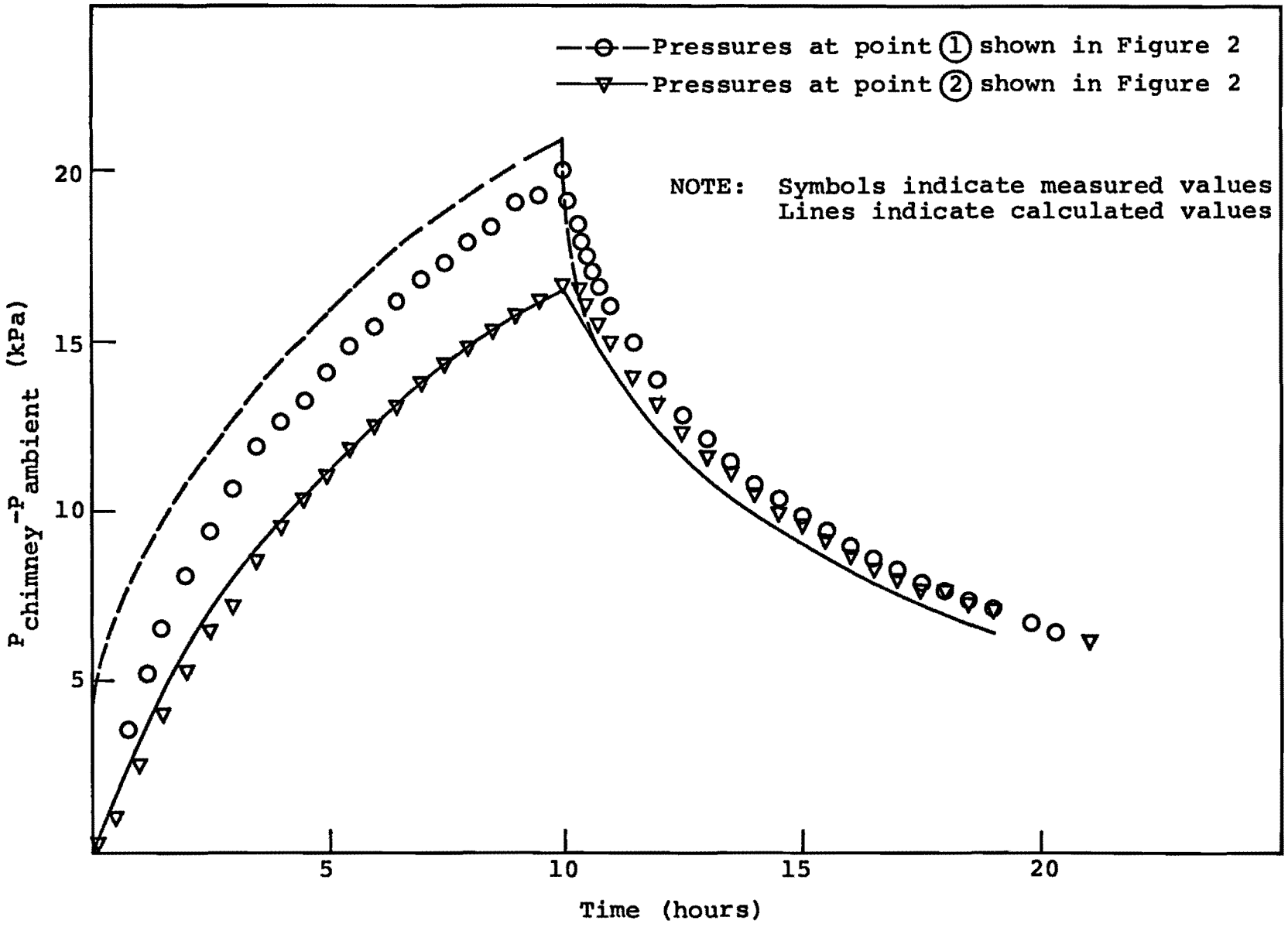

Figure 26 - Comparison of calculated and measured chimney pressure histories using material properties shown in Figure 25.

Results shown in Figure 27 are included to demonstrate the sensitivity of the calculations to small changes in the assumed material properties. For this calculation, the material properties were assumed to be identical to those shown in Figure 17 with the exception that the effective permeability and accessible void fraction of the paintbrush and upper chimney materials were reduced 10 percent (see Table 4). These small changes in assumed material properties are seen to result in calculated pressures which deviate significantly from the measured values. The demonstrated sensitivity is not meant to infer that material properties have been determined to within 10 percent accuracy. They are obviously also dependent on the accuracy to which the chimney geometry can be determined from 3 drill holes. However, because of the sensitivity of the calculations, selected material properties should be accurate to within factors of 2 or less.

Numbers of sets of material properties yield calculations which reproduce the general shape of the data during both pressure rise and decay. However, only two types of material property distributions provide correct pressure equilibration rates within the chimney. The first and most representative is that presented in Section 5.2 where a large accessible void fraction was assumed to occur in the injection region or middle portion of the chimney. This makes available, within the chimney, a large source of gas capable of maintaining the observed pressure differences. Another possibility is that discussed in the description of the Ming Blade results.[5] In that case, it was postulated there existed a layer of material positioned somewhere between the injection and top chimney regions having a relatively low permeability. This low permeability layer decreases communication between these points and effectively lengthens the time required to attain pressure equilibrium. Because the communication between the injection

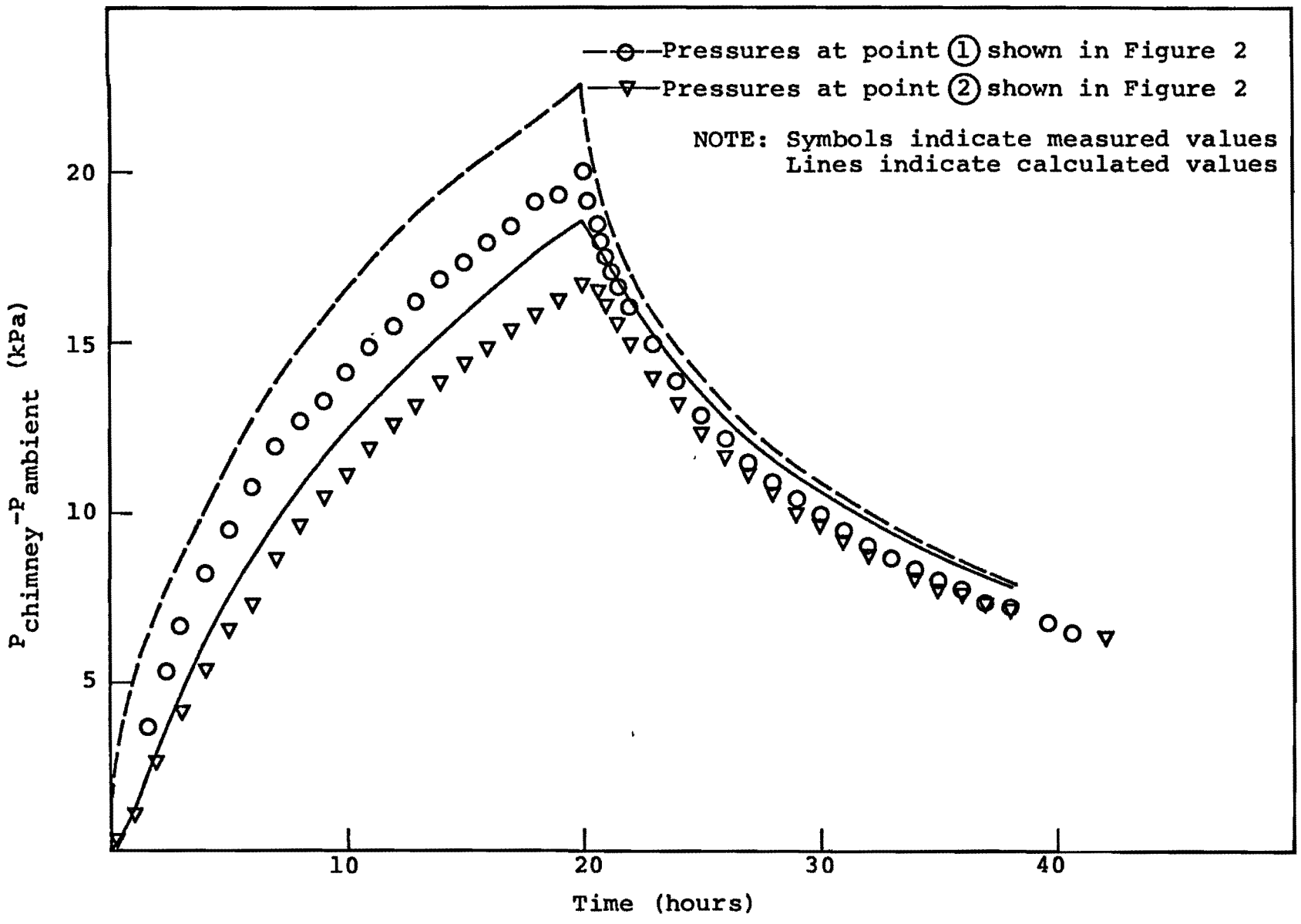

Figure 27 - Comparison of calculated and measured chimney pressure histories illustrating the sensitivity of the calculated results.

region and the top of the chimney is very rapid during the pressure rise period, a low permeability layer cannot exist in the Dining Car chimney. Changing the distribution of material properties within the paintbrush or tunnel bed materials surrounding the chimney will have little effect on the pressure equilibration rate within the chimney since the effective permeability of the chimney material is much higher than that of the surrounding materials.

6. SUMMARY

During the Dining Car tracer-gas chimney pressurization studies, gas flow from the chimney to the tunnel complex and mesa was examined. Air containing a tracer gas was injected into the chimney. Gas samples were collected on the mesa and in the tunnel complex. These samples were analyzed to determine if any tracer gas reached the sampling positions. The absence of tracer gas in the collected air samples indicates there was no gas flow from the Dining Car chimney to the mesa or into the tunnel complex during this test.

Pressures and tracer gas arrival times were monitored within the chimney at points of interest. These results were used to determine material properties. The upper portion of the chimney was found to have an effective permeability of 100 darcies and an accessible void fraction similar to that of the adjacent paintbrush material. Significant bulking occurred in the middle portion of the chimney where the material was estimated to have an accessible void fraction and effective permeability of 0.3 and 150 darcies, respectively. The lower portion of the chimney was found to have a low permeability similar to that expected in the tunnel bed tuff. An analytical-numerical model was developed which accurately predicts pressures within the chimney given the gas injection rate.

A short pressurization test was conducted to determine the ability of the Dining Car chimney to contain the volume of non-condensible gases expected to be produced during the Hybla Gold event. When three times this volume of gas is introduced into the Dining Car chimney, the resulting pressure increase is negligible and there is no indication the gas escapes to the mesa or to the tunnel complex.

REFERENCES

1. Peterson, E., et al., "Gas Flow Calculations for the Ming Blade Chimney - Preliminary Calculational Results," Systems, Science and Software report SSS-R-76-2170, November 1975.

2. Shapiro, A. H., The Dynamics and Thermodynamics of Compressible Fluid Flow, The Ronald Press Company, 1953.

3. Wilson, E. L. and R. E. Nickell, "Application of the Finite Element Method to Heat Conduction Analysis," Journal of Nuclear Engineering and Design, pp 276-286, 1966.

4. Bear, J., Dynamics of Fluids in Porous Media, American Elsevier Publishing Co., Inc., New York, 1972.

5. Peterson, E., personal communication to C. Keller, "Sensitivity of Porosity and Permeability Predictions," 6 October 1976.

APPENDIX I

A complete set of results showing the tracer gas concentrations detected in air samples collected on the mesa during the 24 January test is presented here. Air samples were collected at all positions shown in the figures. These positions correspond to the mesa grid defined in Figure 5 of the report. The numbers shown indicate the approximate Freon 13B1 concentration (x 10^{-11}). The B and C units identified on the figures refer to the two gas chromatographs used to analyze the air samples. Results of a rough analysis, not reported here, indicate that only a small fraction (<0.01 percent) of the gas injected into the chimney seeped to the mesa.

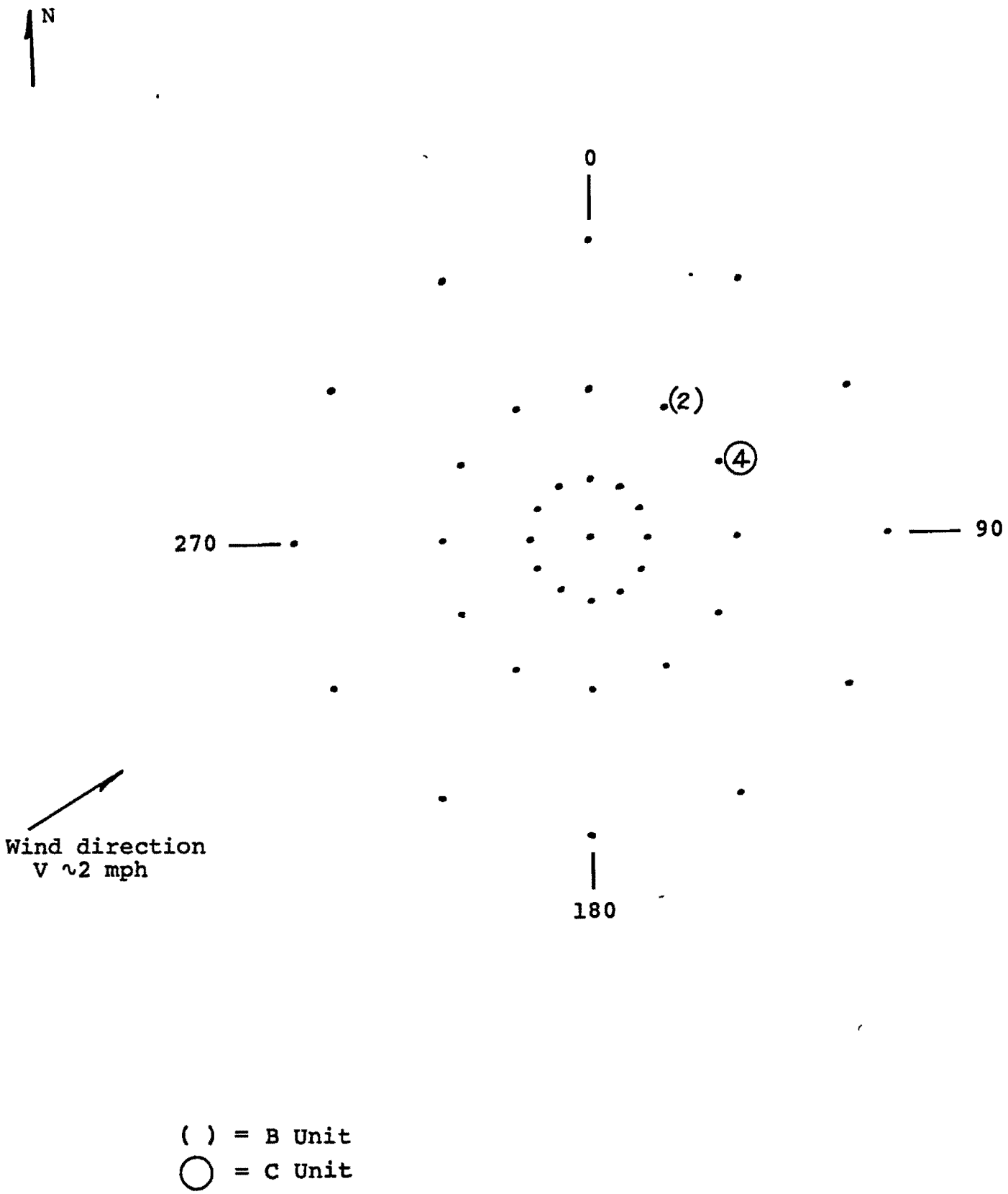

( ) = B Unit

◯ = C Unit

Figure A.1 - Results of analysis of air samples collected on the mesa at 0900 on 26 January 1977.

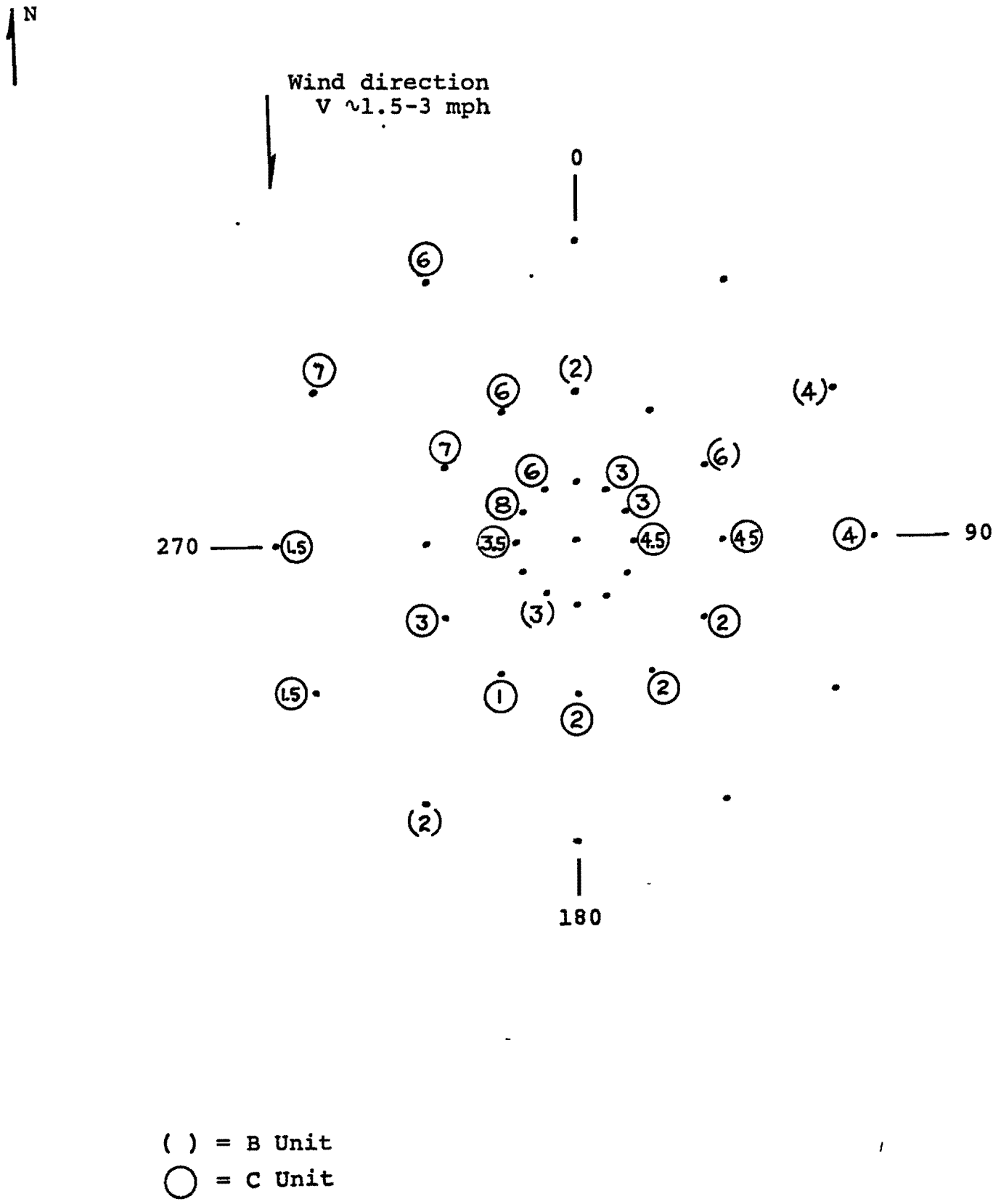

Figure A.2 - Results of analysis of air samples collected on the mesa at 1400 on 26 January 1977.

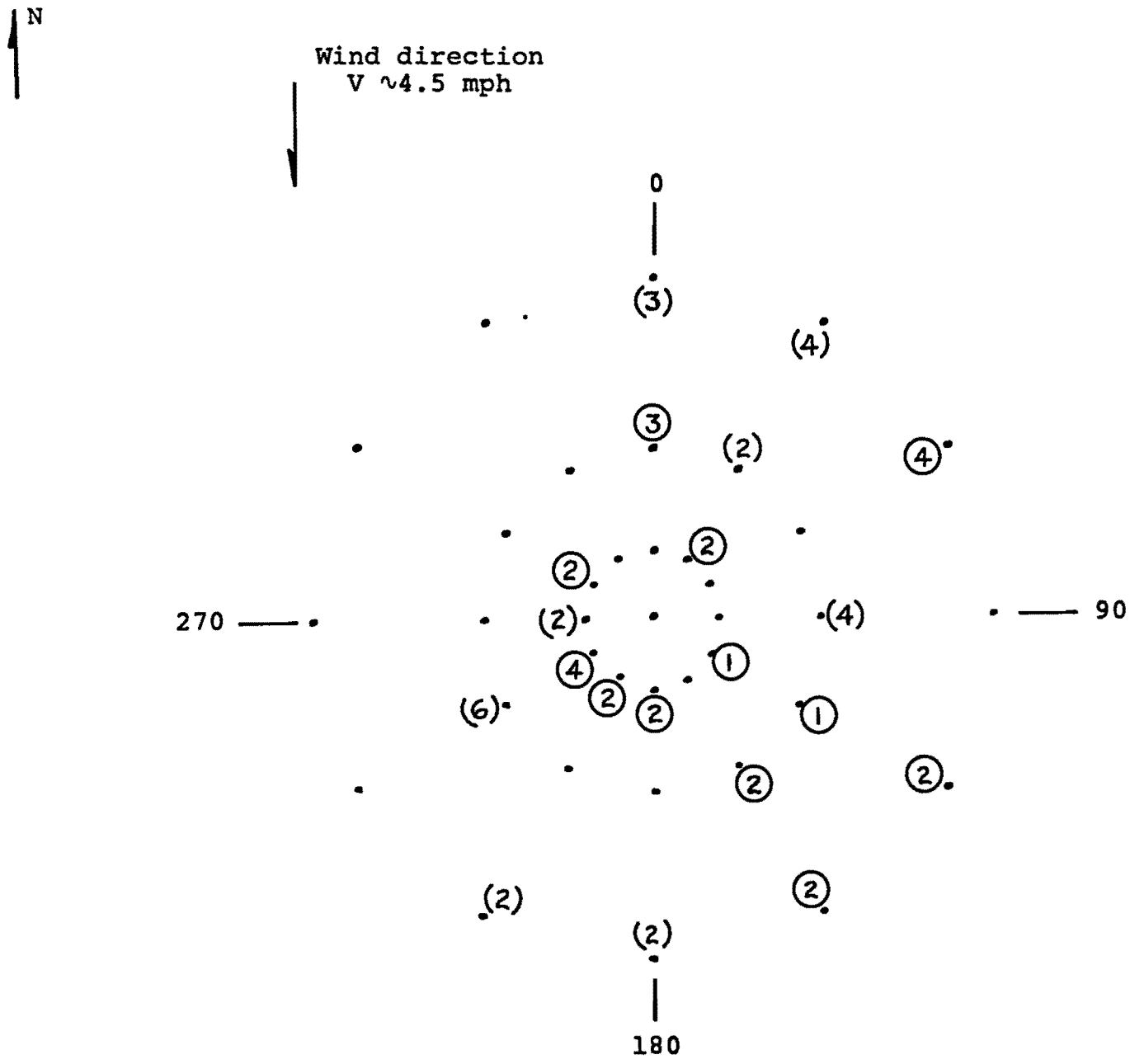

Figure A.3 - Results of analysis of air samples collected on the mesa at 0800 on 27 January 1977.

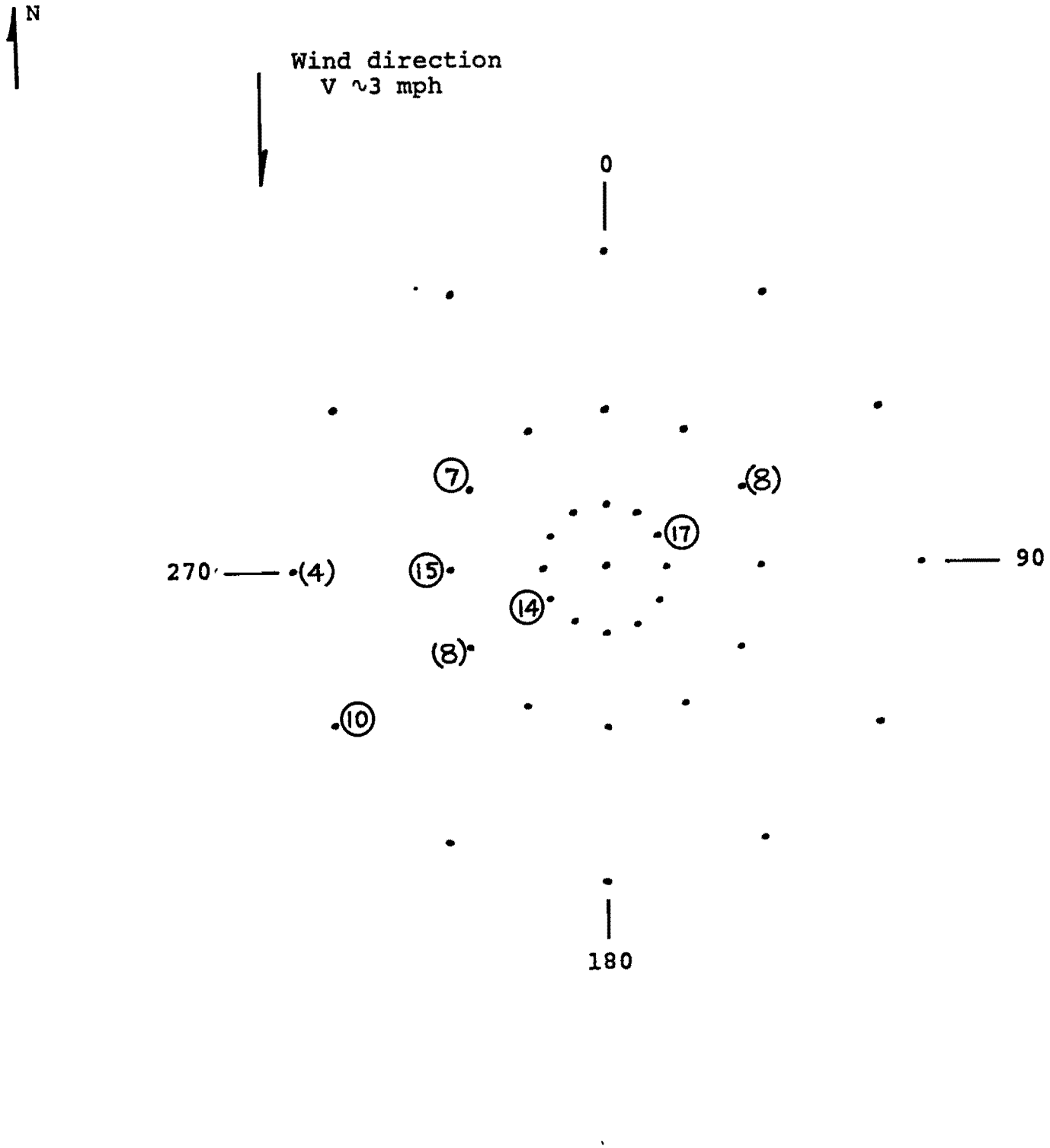

( ) = B Unit

◯ = C Unit

Figure A.4 - Results of analysis of air samples collected on the mesa at 1000 on 27 January 1977.

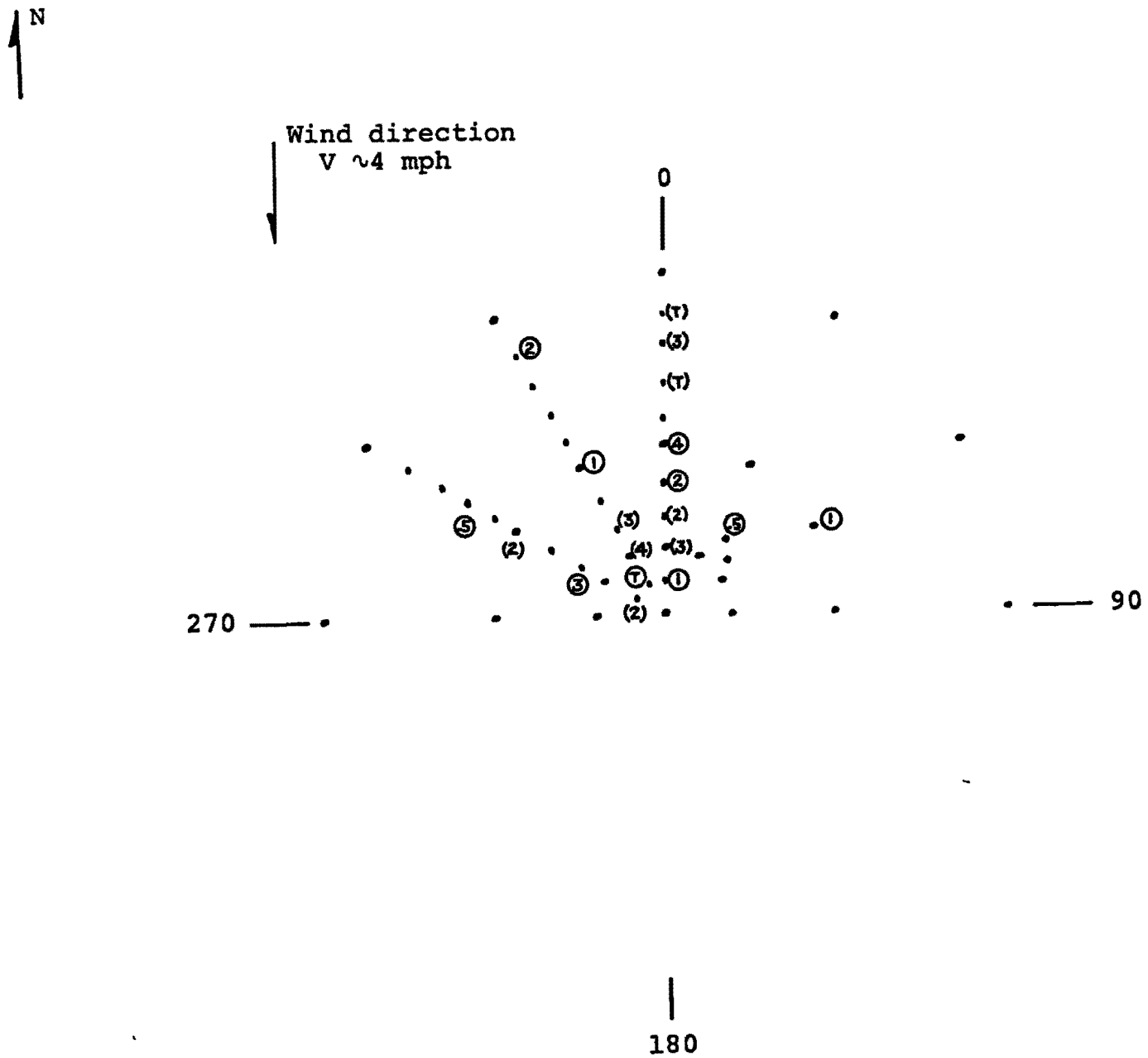

Figure A.5 - Results of analysis of air samples collected on the mesa at 1200 on 27 January 1977.

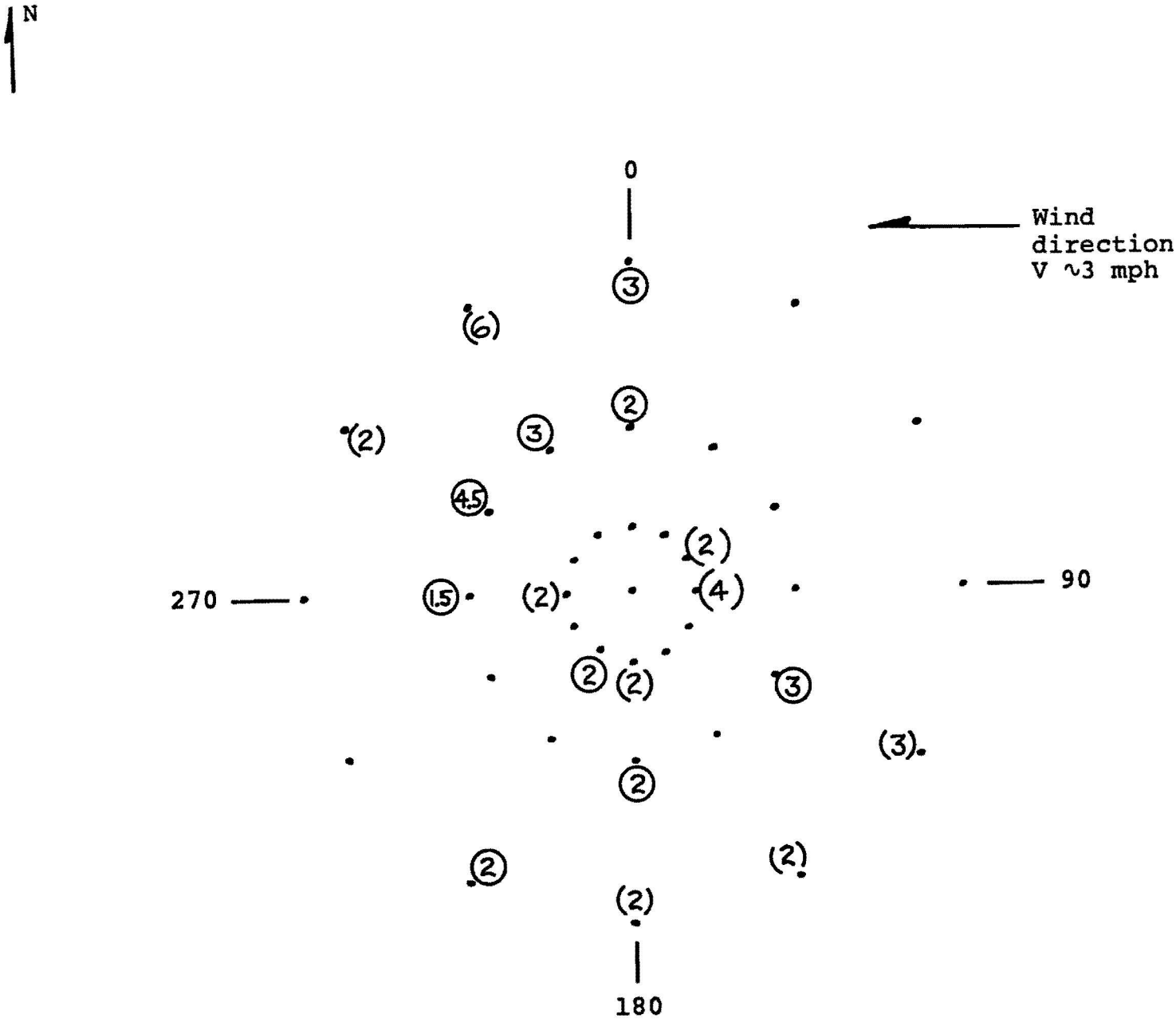

( ) = B Unit

◯ = C Unit

Figure A.6 - Results of analysis of air samples collected on the mesa at 1400 on 27 January 1977.